ČESKÉ VYSOKÉ UČENÍ TECHNICKÉ V PRAZE

Fakulta dopravní

Ústav letecké dopravy K621

Factors defining the brightness of particle images in PIV-application

Faktory ovlivňující jasnost značkovacích částic při měření metodou PIV

Master Thesis

Study programme: Technology in Transportation and Telecommunications

Study field: Air Traffic Control and Management

Master`s thesis supervisor: Dr.-Ing. Peter Scholz; Ing. Jakub Hospodka, Ph.D.

Bc. Matěj Kiss

Předkládám tímto k posouzení a obhajobě diplomovou práci, zpracovanou na závěr studia na ČVUT v Praze Fakultě dopravní.

Prohlašuji, že jsem tuto diplomovou práci vypracoval samostatně a že jsem uvedl veškeré použité informační zdroje v souladu s Metodickým pokynem o etické přípravě vysokoškolských závěrečných prací.

Nemám závažný důvod proti užívání tohoto školního díla ve smyslu § 60 Zákona č.121/2000 Sb., o právu autorském, o právech souvisejících s právem autorským a o změně některých zákonů (autorský zákon).

V Praze dne ....

podpis autora

Acknowledgement

I would like to express my deepest gratitude to my supervisor Dr.-Ing. Peter Scholz, for providing me the opportunity to work on such an interesting research topic and also being so supportive at all times during the project. I am also deeply grateful to Ing. Yosef El-Sayed for his endless help during my whole stay at the ISM, for his support and enthusiasm. This thesis would also not be possible without Ing. Jakub Hospodka, Ph.D., who helped me to realize the whole project abroad. I cannot forget to mention many who helped me with tasks I struggled with and who gave me a so much needed push: Serhat Can, Stephan Loges, Dirk Rabe and many others.

At last but not least, I would like to thank my whole family and friends for their support.

Abstract

Particle Image Velocimetry (PIV) is nowadays one of the leading methods in experimental aerodynamics. The crucial factor for good results is the choosing of the proper particle sort. The objective of this work is to obtain experimental data for images of particles when using PIV method, especially of their brightness, scattering properties or signal-to-noise ratio. This is achieved by thoroughly measuring several particle sorts` behaviour under numerous conditions, such as various laser power, amount of seeding, laser sheet thickness, size of AOI, camera angle, aperture settings, camera lenses, concentration of seeding and depth of water between the camera and the laser sheet.

Key words: PIV, Particle image velocimetry, Seeding, Tracing particles, Particle brightness, Particle size, AOI, Laser power, Laser sheet thickness

Bibliographical reference: KISS, Matěj. *Factors defining the brightness of particle images in PIV-applications*. Prague: Czech Technical University in Prague, Faculty of Transportation Sciences, 2016. 78 pages. Supervisor(s): Dr.-Ing. Peter Scholz; Ing. Jakub Hospodka, Ph.D.

Table of contents

1. Introduction

A need to study behaviour of a fluid flow is as old as fluid mechanics itself. This (**Figure 1**) famous picture of Ludwig Prandtl depicts the German engineer standing next to an original water test tunnel he himself designed. It was used to study aspects of unsteady separated flows behind various obstacles. With this device he was able to study two-dimensional models of profiles under different conditions by simply placing the model vertically into the tunnel and distributing a suspension of mica particles on the water surface. This complete control over the experiment allowed him to thoroughly study basic features of the flow.

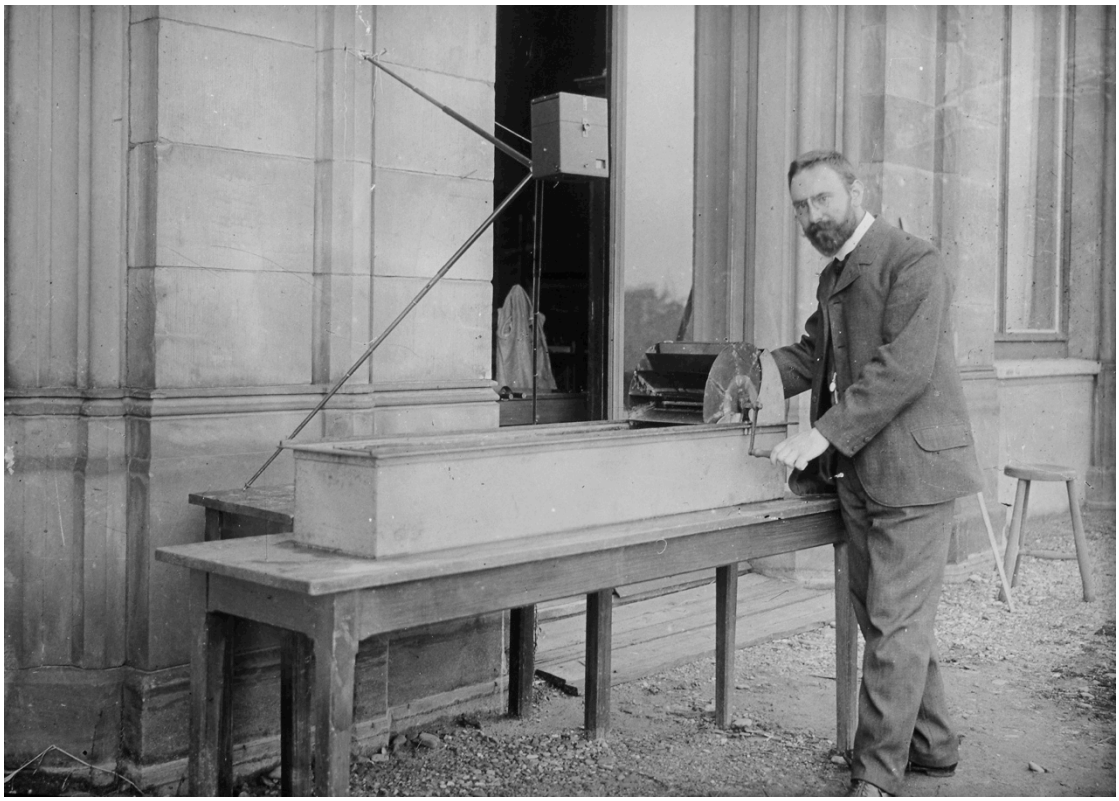

Figure 1 - Ludwig Prandtl (1904) *[Source: Wikimedia commons]*

1.1 PIV Method

However, Prandtl`s tunnel did not allow him to get any quantitative data about the flow velocity, not to mention its velocity at specific areas (vortexes, etc.) in the vicinity of the object. With the evolution of (digital) photography, high-speed cameras and advanced computation algorithms, scientists were able to quantitatively evaluate the flow, nowadays even in real time or in 3D.

A typical experimental setup using Particle Image Velocimetry (PIV) can be divided into few subparts **(Figure 2)**: **Seeding particles** (also known as **Tracer particles**) evenly distributed within the fluid to visualize the flow, **High-power laser** with optics to create an illuminated plane in the fluid parallel to the direction of the flow, **High-speed camera** and also a **Computer** for a data evaluation.

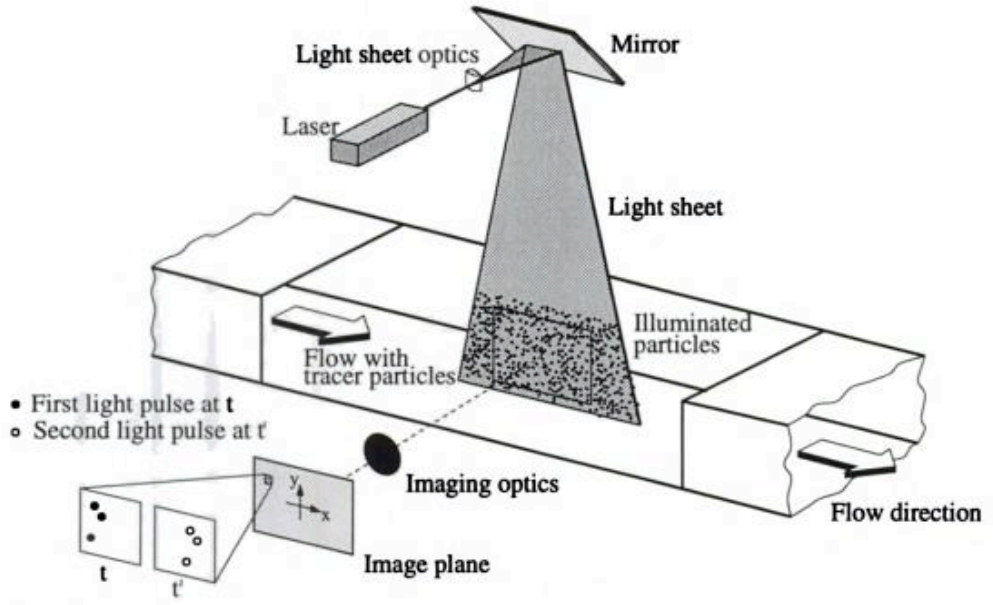

Figure 2 - General PIV setup [1]

A high-speed camera is synchronised with the laser, which means a picture is taken every time the laser goes on. Laser illuminates a plane in the flow twice with a very small delay (this must be set according to the flow velocity). From these double-pictures, the cross-correlation algorithm locates and calculates the shift of each particle. It is assumed that tracer particles move uniformly with the flow during the time between the two images were taken and since the shift in space and time delay are known, algorithm can easily calculate each particle`s speed vector. One of the advantages of PIV is that the measuring equipment has no influence on the flow. Unlike when using other methods, only the presence of tracer particles is needed in the fluid. No pressure probes or other equipment must be built-in within the measuring area. That is, for example, especially vital at high speeds, when shock waves behind such obstacles might significantly influence the results. Under these conditions, PIV method can almost instantaneously produce two-dimensional or even three-dimensional vector field data.

PIV measurements can be done both in wind tunnels and in water tunnels. In the wind tunnel the airflow typically has to maintain a very large speed in order to reach

the same Reynolds number for the (usually) scaled model. Measurements at such speeds require advanced hi-speed cameras and software. But even the distribution of seeding particles into the flow posses a problem. Typical tracing particles for wind tunnels are for example oil droplets. However, the relatively small air density significantly restricts their volume to sizes of around 1 micrometre. And even then they must be inserted into the flow right in front of the model, because they tend to fall down with the gravity.

Wind tunnels are generally more widely used, however water offers many advantages especially when using PIV. Thanks to the higher density of water, the speed of the flow is relatively small and also the seeding size is not that restricted. On the other hand, high forces generated by a model of a wing require use of strong materials (lift of the model with a wingspan=1m and a basic flap at 60 deg. at the v=6 $m.s^{-1}$ was roughly 20 000 N).

According to the density of tracer particles, it can be distinguished between three methods of PIV:

- Low density – individual particles can be distinguished and identified on images. This method is referred to as “Particle Tracking velocimetry” (PTV).
- Medium density – individual particles can be still detected, however it is not possible to detect image pairs by visual methods only, but it requires application of statistical techniques. This method is referred to as PIV.
- High density – individual particles cannot be detected any more because they may even overlap on the image and form flecks (speckles). This method is referred to as “Laser Speckle Velocimetry” (LSV). [1]

1.2 Seeding Particles

The obtained particle image intensity and the contrast of the PIV recordings are directly proportional to the scattered light power. During wind- or water-tunnel experiments, light is for various reasons relatively scarce. Among others, high-speed flows require very short light impulses in order to record sharp double images. The non-optimal position of a camera might lead to a need of increased depth of field (higher *f*-number). It is therefore often more effective and economical to increase the image light intensity by properly choosing the scattering particles than by increasing the laser power.

PIV is an indirect velocity measurement technique – first the particle image shift in time is measured, then the speed of flow is calculated from the velocity of tracer particles evenly distributed in the fluid. For this reason, their careful selection is essential

for good results. [1] Seeding products from two producers, *LaVision GmbH* and *Dantec Dynamics GmbH* are nowadays in use at the Institute of Fluid Mechanics (Institut für Strömungsmechanik) at TU Braunschweig. For the purpose of this thesis, only products from these producers were taken into account **(Table 1)**. This work also focuses solely on the use of PIV technique in water; other types of seeding particles are not considered.

Table 1 - List of examined sorts of particles

LaVision GmbH	**Dantec Dynamics GmbH**
Vestosint 20 µm (VEST20)	Polyamide Seeding Particles 5 µm (PSP05)
Vestosint 55 µm (VEST55)	Polyamide Seeding Particles 20 µm (PSP20)
Vestosint 100 µm (VEST100)	Polyamide Seeding Particles 50 µm (PSP50)
Glass Hollow Spheres 20 µm (HGS20)[1]	Glass Hollow Spheres 10 µm (HGS10)
Glass Hollow Spheres 75 µm (HGS75)[1]	Silver Coated Glass Hollow Spheres 10µm SHGS10

1.2.1 Polyamide Seeding Particles (PSP)

Micro porous particles produced by polymerisation process with round, but not exactly spherical shape. Polyamide 12 (PA 12) powders are used for metal coating, production of fibre composite materials and are for example used as additives to improve the quality of coating of wires. The theoretical maximum upper size of particles is 250 microns. They are highly recommended for water flow applications. [2] [3]

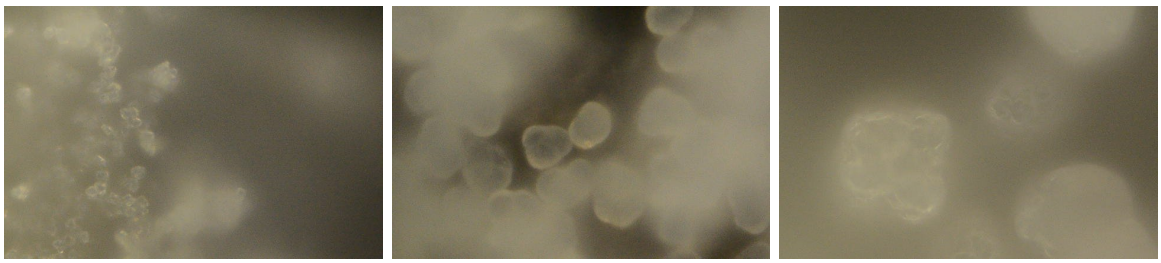

Figure 3 - Pictures of PSP05, PSP20, PSP50 (left to right; all 100x)

[1] Not in the official Product list of LaVision. According to Mr. Knut Mannel, Sales & Application Engineer by LaVision, both sorts were only samples sent by their manufacturer to LaVision Company. LaVision later decided not to add them to their portfolio.

1.2.2 Vestosint

VESTOSINT® is a registered trademark of particles based on polyamide 12 (PA 12) produced in Germany by *EVONIK Degussa GmbH* company and sold by *LaVision*. [4]

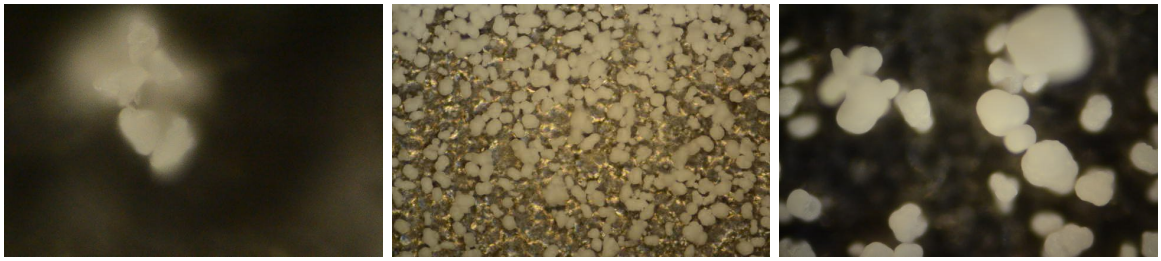

Figure 4 - Pictures of VEST20 (100x), VEST55 (10x), VEST100 (20x) (left to right)

1.2.3 Hollow Glass Spheres and Silver Coated Hollow Glass Spheres

Borosilicate glass particles with a spherical shape and a very smooth surface, preferably for liquid flow applications. The thin silver coating further increases the reflectivity.

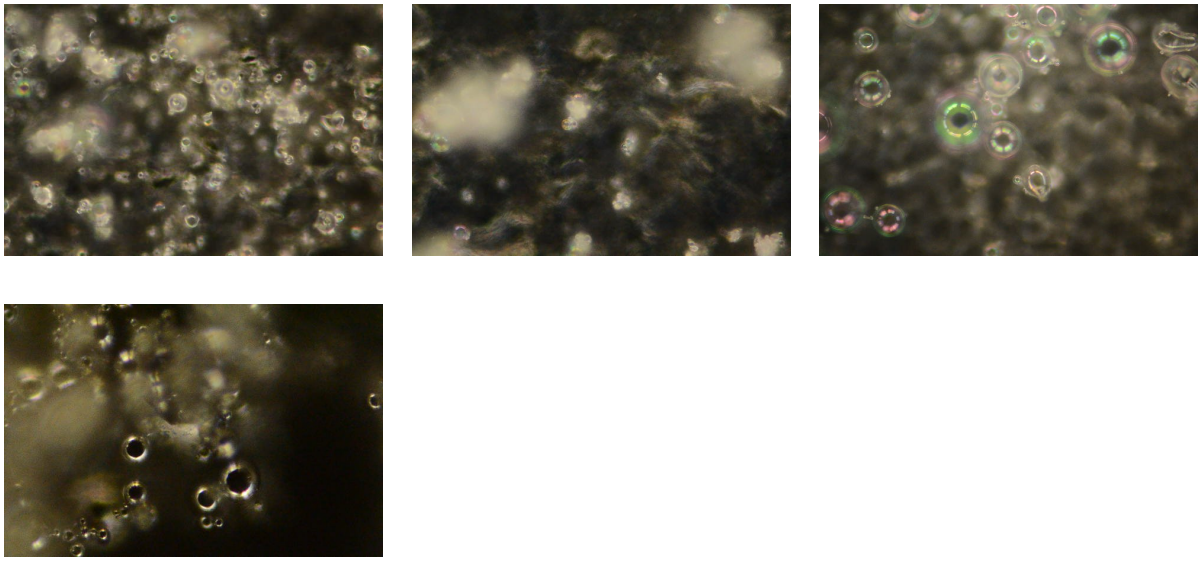

Figure 5 - Pictures of HGS10 (50x), HGS20 (50x), HGS75 (20x) and SHGS10 (100x)

Table 2 - Properties of examined particle sorts

	PSP	VEST	HGS	SHGS
Mean particle diameter (µm)	5, 20, 50	20, 55, 100	10, 20, 75	10
Size distribution	1-10 µm 5-35 µm 30-70 µm	-	2-20 µm	2-20 µm
Particle shape	Non-spherical, but round	Non-spherical, but round	Spherical	Spherical
Density (g/cm3)	1,03	1,23; 1,2; 1,0-1,2	1,1	1,4
Refractive index	1,5	- (1,5?)	1,52	-
Material	Polyamide 12	Polyamide 12	Borosilicate glass	Borosilicate glass
Price	164,00€/250g (65,60€/100g)	90,00€/500g (18,00€/100g)	75,00€/250g (30,00€/100g)	228,00€/100g

1.3 Criterion of Choosing Proper Seeding Particles

As mentioned above, the received particle image intensity is directly proportional to the scattered light power. It can be more effective to increase the image light intensity by properly choosing the scattering particles than by increasing the laser power. This can be easily achieved by increasing the particle diameter and thus a scattering cross section of a particle. **Figure 6** shows such relation between the scattering cross section of a particle and a ratio of particle size to wavelength.

However, it must be noted that the increase of a particle size is connected with changes in its physical properties. At first, scattering regime changes and therefore also changes the intensity of scattered light under various viewing angles (see Chapter 2). Another source of error is the so-called “velocity lag” caused by the influence of any forces applied on the particle. This can be gravitational force induced by the difference between particle density and the fluid density or particle inertia caused by a rapid change of flow direction. The induced velocity can be derived from Stoke`s drag law. For gravitational component yields:

$$U_g = d_p^2 \frac{(\rho_p - \rho)}{18\mu} g \qquad (1)$$

where μ is the dynamic viscosity of the fluid, g is the acceleration due to gravity and d_p is the particle diameter. Using (1), velocity lag for constantly accelerating fluid can be further derived. The problem and the equations are further discussed in [1].

This typically does not pose a problem for liquid flows where the particle density usually varies around 1,0 - 1,4 g/cm^3, but it should be noted that particle velocity typically follows an exponential law for much greater density difference. Hence it is desirable to keep their (practically unavoidable, but yet small) difference at its smallest. Not complying with that might cause data drop-out in critical areas such as boundary layers, vortex cores, etc.

Table 3 - Seeding materials for liquid flows

Type	**Material**	**Mean diameter (μm)**
Solid	Polystyrene	10 – 100
	Aluminium flakes	2 – 7
	Hollow glass spheres	10 – 100
	Granules for synthetic coatings	10 – 500
Liquid	Oils	50 – 500
Gaseous	Oxygen bubbles	50 – 1000

It can be seen that particle diameter should be big enough to supply satisfactory light scattering characteristic but yet small to ensure good tracking of the fluid motion. Therefore, it is clear that a compromise has to be found. Table 3 shows the most common seeding materials for liquid flows. [1] Great advantages of solid particles are their constant properties over time. Unlike in a case of wind tunnels, their insertion into a water tunnel can be relatively easily done and their amount can be easily measured.

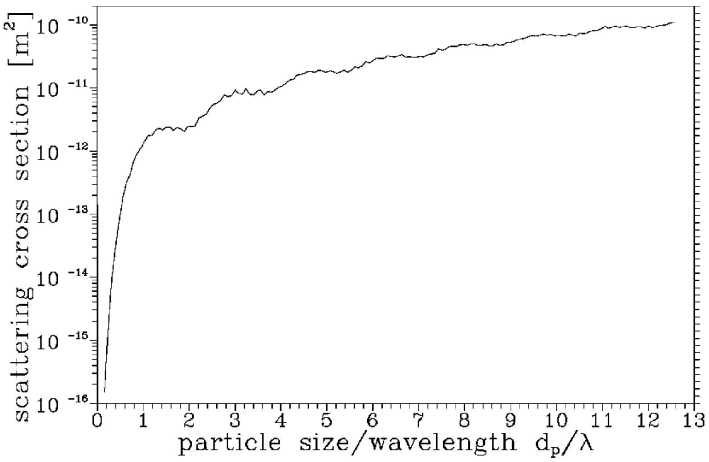

Figure 6 - The scattering cross section as a function of the particle size to wavelength ratio (Refractive index m=1.6). [5]

2. Theoretical Background

2.1 Extinction

Hardly ever is light observed directly and only from its source. When watching objects we meet everyday in our environment, we usually see reflected sunlight (or other light source) – that is most of the light reaches our eyes in an indirect way. Even an old-fashioned light bulb does not send its light directly from its source (luminous filament), but shows the scattered light by its glass bulb.

The process of removing energy from light is called *Extinction*. For the purpose of easier understanding, this work will follow the terminology used in [6], i.e.:

$$\text{Extinction} = \text{scattering} + \text{absorption} \tag{2}$$

As we can see, there are two processes accompanying each other. First is the *Absorption* of light, which is for example responsible for our perception of colours (grass is green because all other wavelengths/colours of the incident light are absorbed and turned into other energy (what form of energy is for the purpose of this work now irrelevant). Absorption prevails in very dark materials such as coal or asphalt and is on the other hand nearly absent in clouds at visual wavelengths. But it is the other process, *Scattering,* that prevails in clouds at visual wavelengths (higher frequencies such as microwaves penetrate clouds easily). As the sunlight enters the cloud, its beams scatter by liquid droplets in all direction. The best example of light scattering is the change of colour of the clear sky during the day. At noon it is purely blue, only to change into red at the sunset. It is because in the morning/evening sunlight has to follow much longer path through the atmosphere to the observer. As the shorter wavelengths (violet and blue ~475 nm) are scattered more efficiently than longer (orange, red ~650 nm), almost only red tones reach the observer.

For the purpose of this work it is assumed that the scattered light has the same frequency as the incident light. Any quantum transitions effects are excluded.

2.2 Dependent and Independent Scattering

It must be noted that if light enters a perfectly homogeneous medium, it would not be scattered. Molecules of a perfect crystal at absolute zero would be arranged in a regular way so that the waves scattered by each molecule would interfere in such a way as to cause no scattering at all but only a change in the velocity of propagation.

This is an ideal case; in an actual fluid a random arrangement of molecules causes a real scattering. Whether or not the molecules are arranged in a regular way, the final result is always a cooperative effect of all molecules. However, it is the distance between the molecules, which matters. According to [6], sufficient condition for independent scattering is average distance of 3 times the radius. For instance, even a very dense fog consisting of droplets 1 mm in diameter and through which light can penetrate only 10 meters has about 1 droplet in 1 cm^3, which means that the average distances are approximately 20 times the radii. Since the diameter of particles used for experiments in this work is at least 10^3-times smaller and their distance in n-times larger, we can assume the scattering to be independent.

2.3 Single and Multiple Scattering

The obvious assumption for a solution containing N particles is that the scattered intensity is N times that scattered by a single particle and that the extinction (energy removed from the original beam) is also N times that removed by a single particle. However, this proportionality holds only if the radiation to which each particle is exposed is essentially the light of the original beam. Only a certain number of particles are exposed to the light beam emitted from its source, whereas the rest are exposed to the scattered light AND the light with lower intensity because of the extinction. If this effect is strong, we speak of *multiple scattering* and a simple proportionality does not exist any more. This can be illustrated by a white cloud in the sky, which is basically as a dense fog mentioned above (its droplets are independent scatterers). But the total intensity scattered by the cloud is not proportional to the number of droplets contained, because each droplet is not illuminated by the full sunlight. Droplets further in the cloud receive no direct sunlight at all but only diffused light scattered by other droplets. Thus the light emerging from the cloud has been scattered at least by two or more droplets. For a very thick cloud it is estimated that only about 10% of light intensity emerges after a single scattering.

Multiple scattering does not present any new problems for the independence principle presented above. It stated that each particle can be thought to be independent if exposed to light from a distant source. It is still true whether the source is the sun, laser or another droplet. But the problem of finding the resulting intensity of light in such a multiple scattering scenario is an extremely difficult mathematical problem.

A simple test for the presence or absence of multiple scattering is to double the concentration of particles in the sample. If the resulting intensity is doubled, only

single scattering is important. It will be further seen, that for the experiments listed in this work are effects of multiple scattering essential. [6]

2.4 Light Scattering Behaviour

There are three parameters that govern the scattering:

1. *Wavelength* λ of the incident light
2. Size of the particle, *normalized diameter* [1]

$$q = \frac{\pi d_p}{\lambda} \tag{3}$$

   Where d_p is a particle diameter.

3. The particle optical property relative to the surrounding medium, *Complex Index of Refraction*

$$m(\lambda) = n(\lambda) - ik(\lambda) \tag{4}$$

Where *n(λ)* and *k(λ)* are the *Refractive Index* and the *Extinction Coefficient* respectively (as a function of λ), n can be interpreted as the scattering and k as the absorption part of the equation. For example, a particle with k = 0 would not absorb light, but it will scatter light. In reality it can never be exactly equal to zero, because every material absorbs a little. Theoretical material with such properties as n = 1, k = 0 would be then practically invisible (however not in a way as black holes – fully absorbing the light). Typical values for Refractive indexes of studied materials can be seen in **Table 4 - Properties of examined particle sorts** and ranges around ~ 1,5. Value of the Extinction coefficient for Water (at λ = 532nm) is k = 1,4992x10-9. [7] [8]

For *q* there exist three regimes:

- *q << 1* (the Rayleigh regime): For a particle which is much smaller than the wavelength. The scattering process in this regime can be described by a simplified theory. (See **Chapter 2.4.1**)
- *q = 1*: The particle size is similar to the wavelength. The most complex regime; requires solution using Maxwell equations (Mie theory; **Chapter 2.4.2**).
- *q >> 1* (geometric optics regime): For a particle which is much larger than the wavelength. Scattering is not simpler, but the reflection on the surface and refraction in the interior can be for example calculated using ray tracing through the particle and off the particle's surface. [7]

2.4.1 Rayleigh Approximation

Rayleigh scattering describes the scattering of light by homogenous spheres, which are much smaller than the wavelength of light. This method gives a very good estimate of results and simultaneously its solution is very easy compared to Mie equation. Its use is limited by following:

1) Particle size up to 10% of a light`s wavelength
2) Particles must be randomly positioned in a medium. The scattered light thus arrives at a particular point with a random collection of phases. It is then incoherent and the resulting intensity equals the sum of the squares of the amplitudes from each particle and therefore proportional to the inverse fourth power of the wavelength and the sixth power of its size. This can be fulfilled in gases or in water.

For example, for a visible light with a wavelength between $\lambda_{min} = 400\ \mathrm{nm}$ to $\lambda_{MAX} = 790\ \mathrm{nm}$, we can estimate the maximal size of a particle: [9]

$$\frac{\pi d_p}{\lambda} \ll 1 \quad \Rightarrow \quad d_p \ll \frac{\lambda}{\pi} \quad \Rightarrow \quad d_{p_{MAX}} \approx 0{,}1\ \mu m \tag{5}$$

Size of seeding particles used in this work ranges from 5 μm to 100 μm, which turns the Rayleigh approximation for this paper unfortunately unusable.

2.4.2 Mie Scattering

The Mie solution to Maxwell's equations (also known as *Mie scattering*) describes the scattering of an electromagnetic plane wave by a single homogeneous sphere. It is named after Gustav Mie and can be used for all sizes of spheres. [6] Its solution is more complex than of the Rayleigh approximation, which is why the latter is used whenever possible.

Key assumptions are:

- Particle is a sphere
- Particle is homogenous (= single refractive index) [9]

Mie scattering can be characterized by the normalized diameter *q*, defined by (3). With increasing *q*, the ratio of forward to backward scattering intensity will increase rapidly. Although it would be useful to record in forward scatter in order to record with the maximal intensity, it is physically impossible. Usually an angle of 90° is mostly used.

Mie scattering theory can calculate the scattering phase functions of particles used during the experiment. To compute and visualise it in Matlab, Christian Maetzler`s BHMIE code was used. It is based on Bohren and Huffman`s work [10]. Based on the following inputs: *Particle diameter*, *Wavelength* and the *Complex index of refraction* this function computes so called *scattering functions* S_1 and S_2, which are complex numbers and describe amplitude *and* phase of the scattered waves. According to the Mie theory, four independent scattering matrixes can be derived for spherical particles based on S_1 and S_2:

$$S_{11} = \frac{1}{2}(|S_2|^2 + |S_1|^2) \tag{6}$$

$$S_{12} = \frac{1}{2}(|S_2|^2 - |S_1|^2) \tag{7}$$

$$S_{33} = \frac{1}{2}(S_2^* S_1 + S_2 S_1^*) \tag{8}$$

$$S_{34} = i\frac{1}{2}(S_2^* S_1 + S_2 S_1^*) \tag{9}$$

Author`s own code had to be added to the Christians Maetzler`s core in order to work further with the results. Using result from (6) for

$$\Phi\ (cos\ \theta) = \frac{1}{q} S_{11}\ (cos\ \theta) \tag{10}$$

scattering phase functions of various particles were computed (for $\lambda = 532\ nm$, $k = 1{,}4992x10^{-9}$ for water) as follows [6] [7]:

(NOTE: Intensity in logarithmic scale)

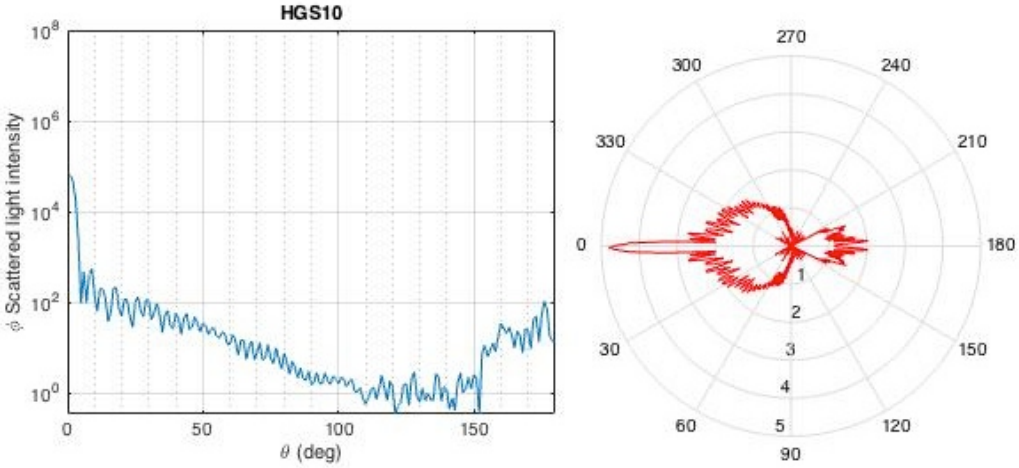
HGS10
ϕ Scattered light intensity
θ (deg)
270
300
240
330
210
0
180
30
150
60
120
90

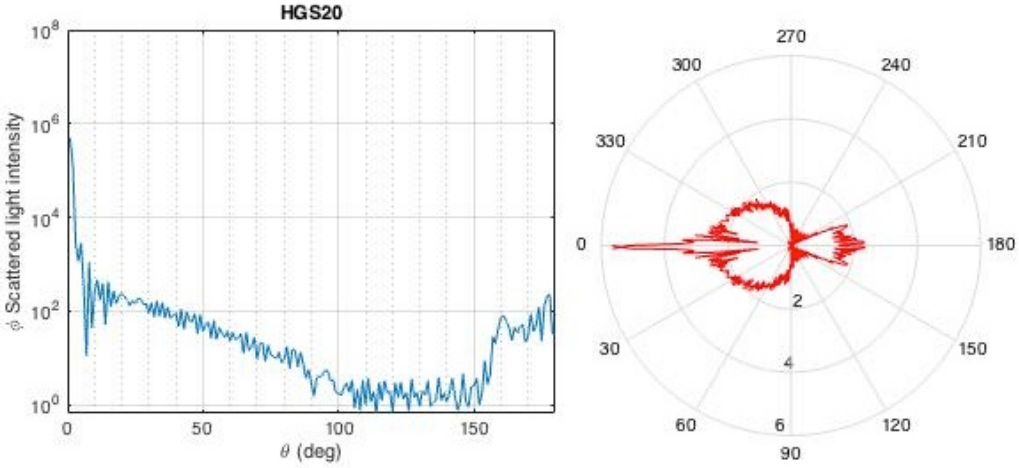
HGS20
ϕ Scattered light intensity
θ (deg)
270
300
240
330
210
0
180
30
150
60
120
90

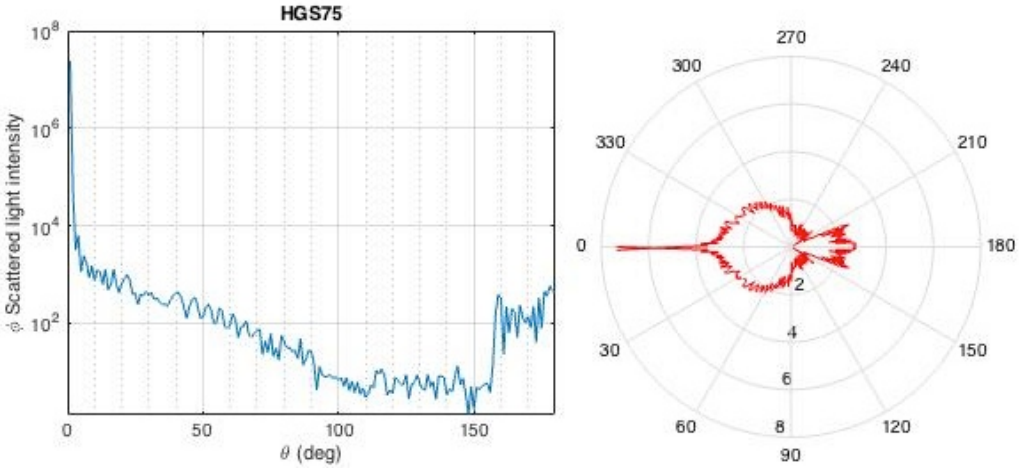
HGS75
ϕ Scattered light intensity
θ (deg)
270
300
240
330
210
0
180
30
150
60
120
90

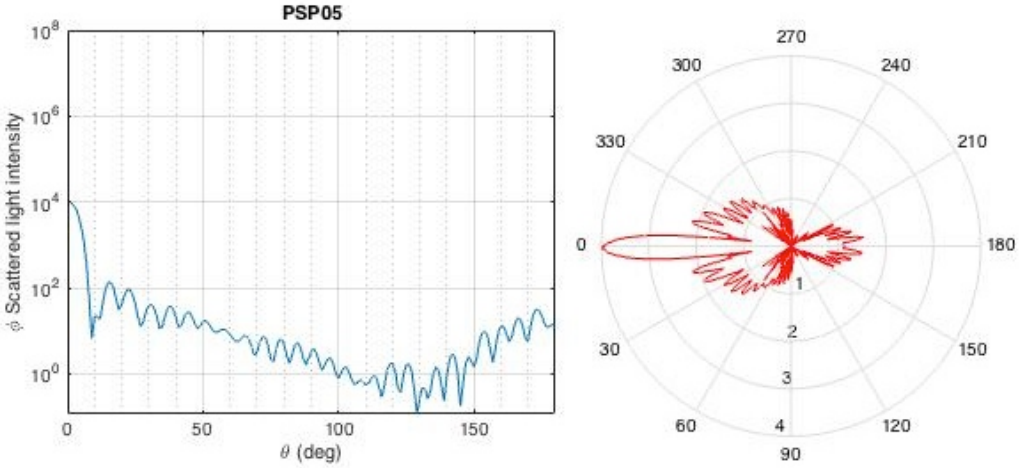
PSP05
Scattered light intensity
θ (deg)

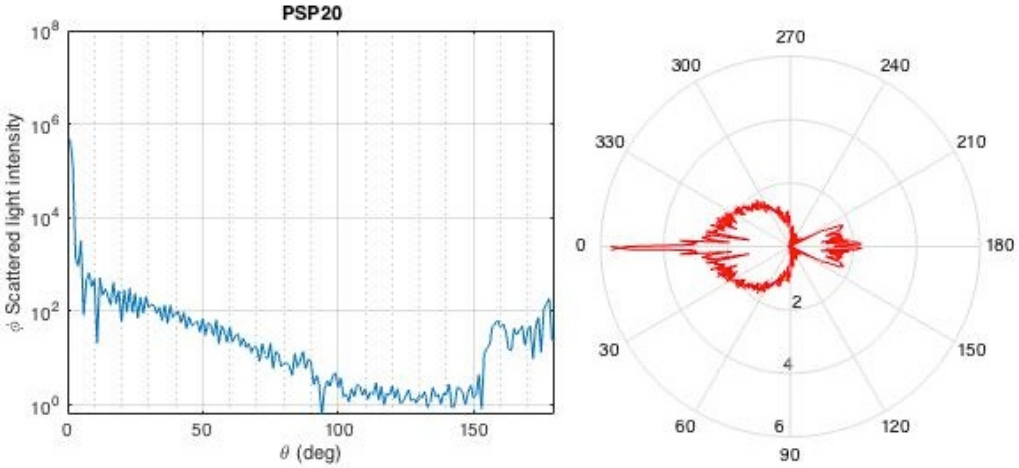
PSP20
Scattered light intensity
θ (deg)

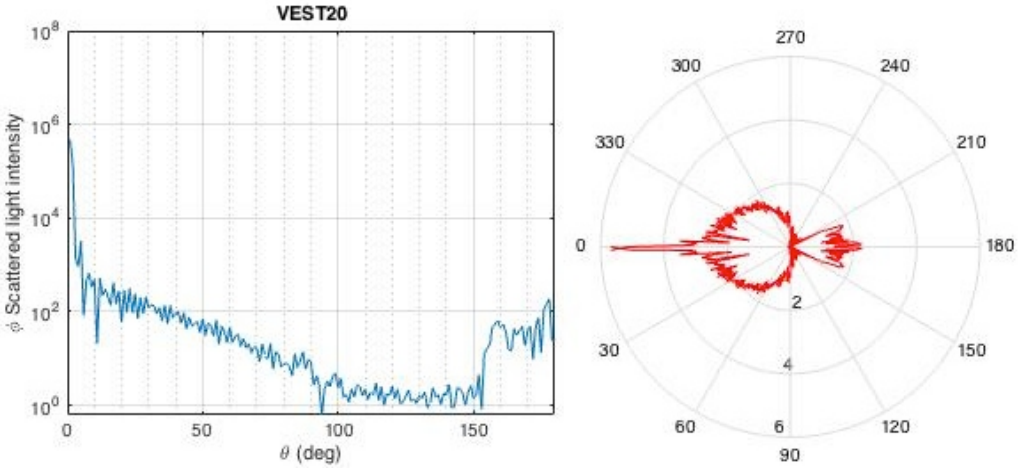
VEST20
Scattered light intensity
θ (deg)

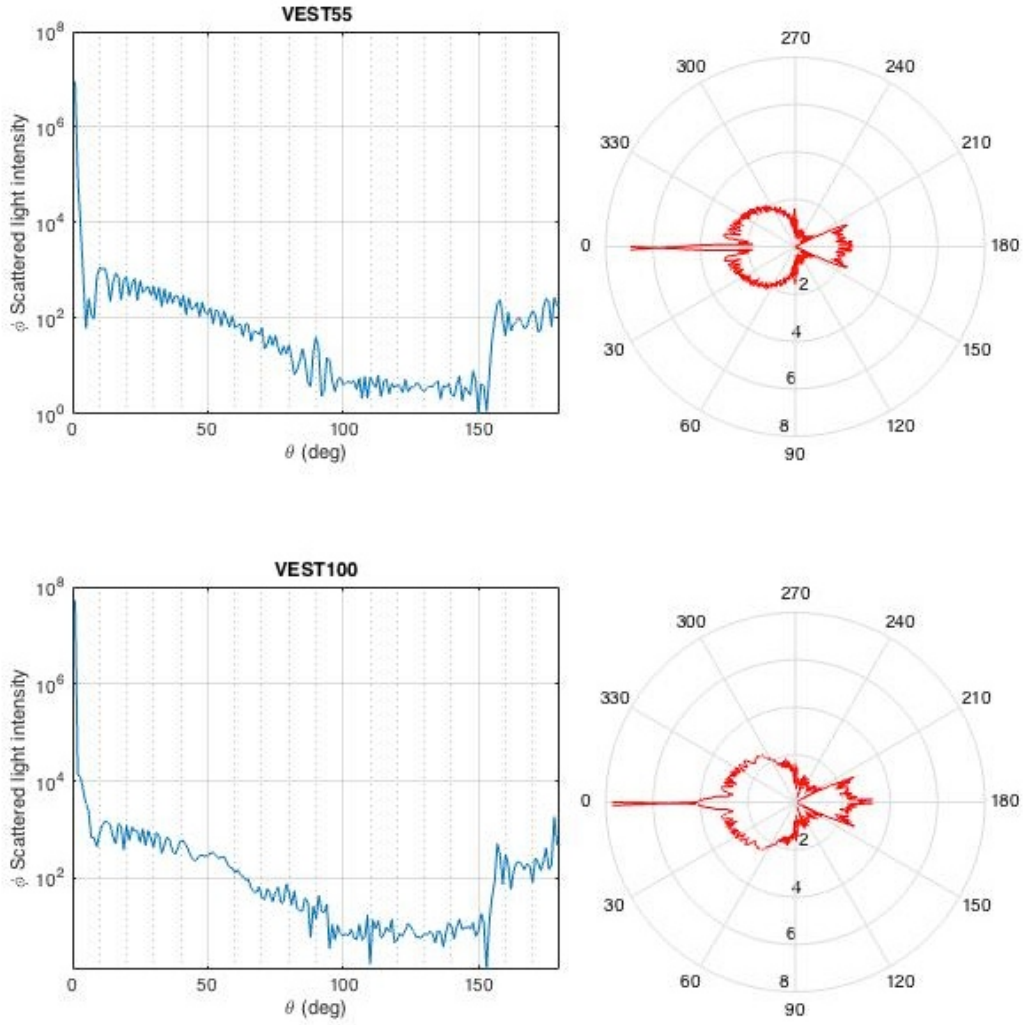

Figure 7 - Scattering phase function of various particles

The results are in accordance with the statement above, i.e. that with an increasing normalized diameter *(q)* ratio of forward to backward scattering intensity increases rapidly. For instance, in case of the smallest seeding sort PSP05 (5 microns) is the ratio $q = 10^4:10^{10} = 1\,000$. By VEST100 (100 microns), which is made from the same material (polyamide P 12 as well) is $q = 10^8:10^3 = 100\,000$.

There is also a tendency for the scattered light intensity to increase with the increasing particle diameter. The number of local maxima and minima is proportional to *q*. It means that the light intensity oscillates rapidly over the changing angle. But when averaging over a range of observation angles, the intensity would be smoothed considerably. The average intensity increases with q^2; the scattering strongly depends on the ratio of the refractive index of the particles to that of the fluid. Since the refractive index of water is larger than that of air, the scattering of particles in air is

about one order of magnitude more powerful than that of the same particles (same size) in water.

In **Table 4** are compared the computed average intensities of light scattered by the particle in all directions and intensities at Φ=90° to find out how much energy is roughly transmitted towards the camera.

It can be seen from all the diagrams, that the particles do not block the incident light, but they spread it in all directions. Therefore, for a large number of particles inside a thin light sheet substantial multiscattering occurs. So the light intensity of a particle imaged by the camera is not only due to direct illumination, but also due to scattered light by other nearby particles. This considerably increases the intensity of an individual particle image in the case of heavily seeded fluids. Particles behind (when looking from the laser) the investigated one are, in other words, due to powerful forward scattering amplifying its image. Therefore a larger number of particles can be used to increase the overall efficiency. On the other hand it is limited due to added background noise on the recording. This scenario will be further studied in following chapters. [1]

Table 4 - Intensities of scattered light for all seeding sorts (Mie scattering)

Seeding	Average scattered intensity (all directions)	Intensity at Φ=90°
HGS10	776	1,57
HGS20	3 335	2,87
HGS75	1 249 100	26,24
PSP05	209	3,45
PSP20	3 496	8,46
PSP50	38 352	14,79
VEST20	3 496	6,84
VEST55	51 161	27,26
VEST100	298 000	28,33

2.5 Transmittance

Transmittance describes the ability of the material to transmit electromagnetic waves, in our case visible light. Total transmittance of a material is defined as a ratio of transmitted light intensity to incident light intensity:

$$T = \frac{I}{I_0} \tag{11}$$

Its value varies for different wavelengths. Transmittance of a clear glass (4 mm thick) for λ = *532 nm* is around $T = 90$. [11]

2.6 Laser Power

Lasers (= “light amplification by stimulated emission of radiation”) usually used for PIV are so called *pulse lasers* (Nd:YAG for example) that emit their energy in short pulses with a higher peak power compared to constant lasers.

3. Experimental Setup

To acquire sets of images under defined conditions, a self-made experimental setup was used. As a construction basis had been used X95 Rail and Carrier System (Newport company); measurements in water were done in a small aquarium (390 x 240 x 220 mm, 4 mm thick glass walls) with a volume of 22 litres. A constant water level for all measurements was kept at 20,592 litres. Use of a smaller water tunnel was also considered, but since studying of a flow itself was not an objective of the measurements, the small aquarium was chosen as a more cost-efficient, eco-friendly and easy-to-handle variant.

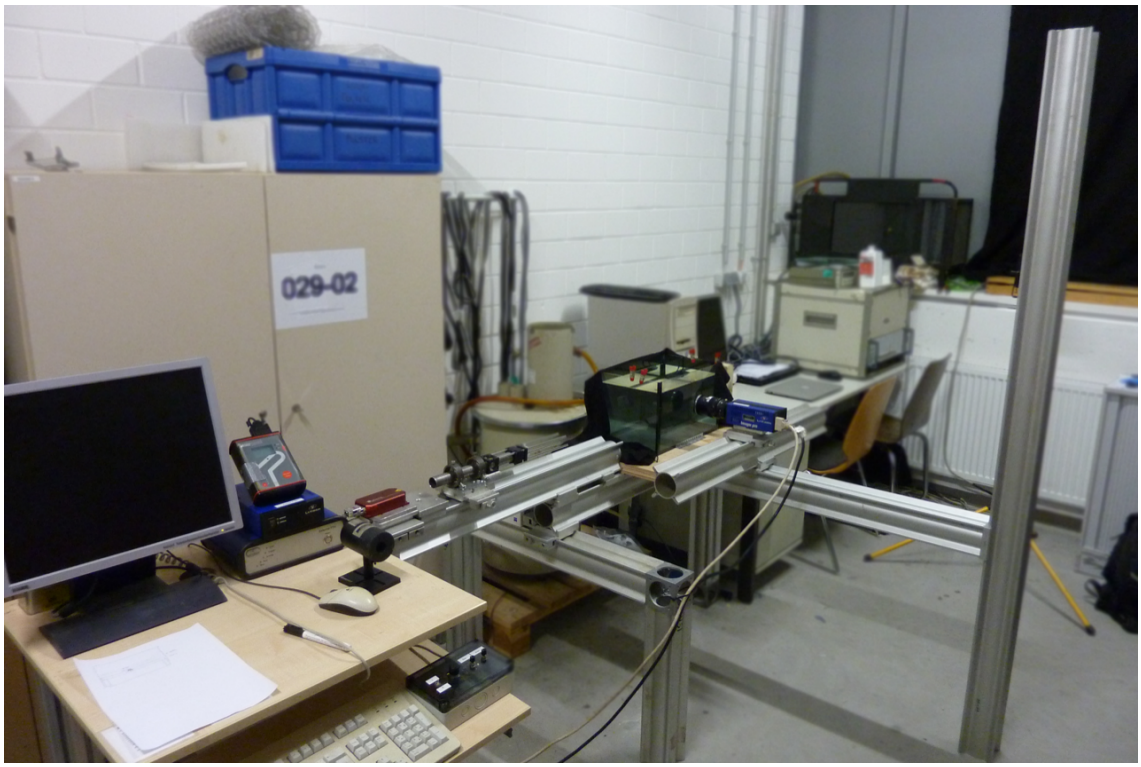

Figure 8 - Setup overview

In **Figure 8** the overview of the experimental setup can be seen. In the left lower corner is a computer with DaVis software, next to it camera control unit, PTU - Programmable Timing Unit (blue boxes next to the computer screen), device measuring the laser power (black tube next to the mouse), laser (small red box), laser optics and the aquarium. In front of it is the camera (blue). It is on the movable arm to enable measurements under angles different from 90 degrees to the laser sheet.

Lights in the room were completely off during the experiments to minimize any light other than laser light. Also heavy curtains were used to cover windows.

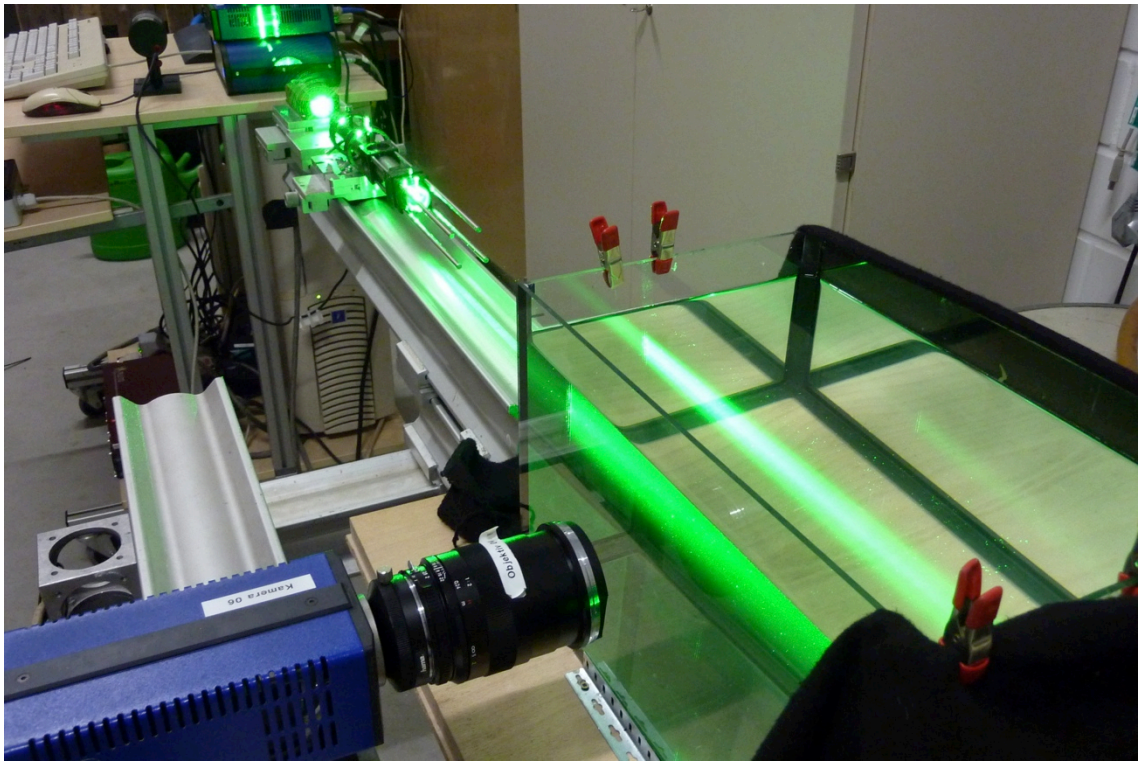

Figure 9 – Setup with the laser on

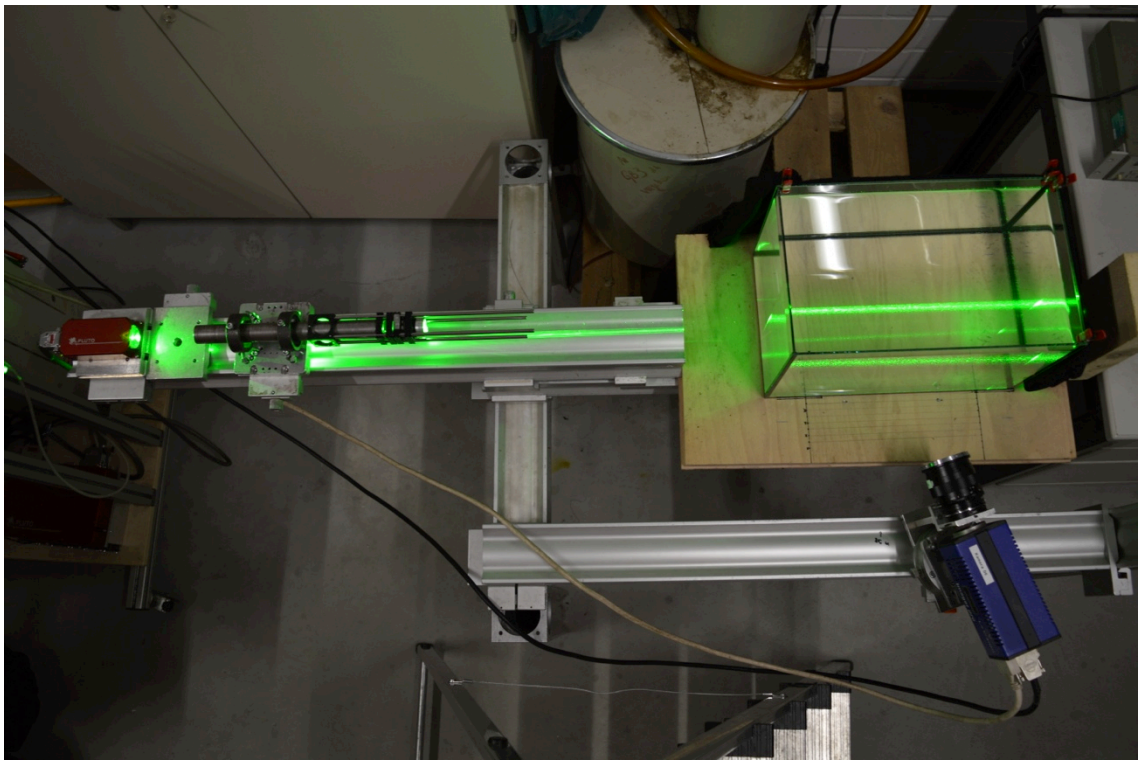

Figure 10 – Top view of setup with installed Scheimpflug adapter

3.1 Measurement Flowchart

For each measurement, following conditions were set, measured and noted:

- Laser power. Measured right in front of the laser (before the beam entered the optics).
- Aperture used
- Shutter speed (controlled in the DaVis controlling program on computer).

Other constants:

- Default AOI (Area of Interest) size = 45 x 36 mm
  (Enlarged AOI size = 63 x 50 mm)
- Camera angle = 90 degrees to the laser sheet plane

3.2 Laser

For the experiment a green Pegasus Pluto-F series Nd-YAG solid-state laser (λ = 532 nm) with a labelled maximal power of 3000 mW (class IV) was used. [5] However, the maximal constantly achievable power during the experiment varied around 2200-2250 mW **(Figure 11)**.

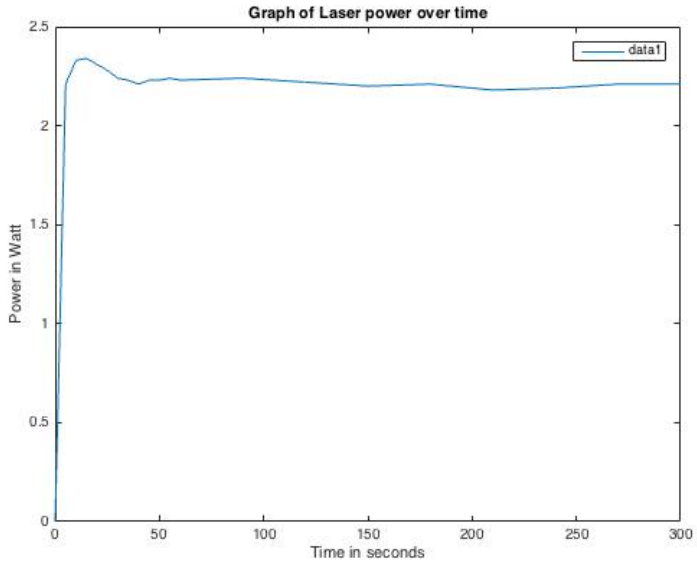

Figure 11 - Laser power over time

Laser power was measured in Watts using Laserpoint Thermal Sensor. Generally, the power of pulse lasers usually used for PIV is measured in Joules per pulse, so it might be desirable to convert Watts using:

$$[Joule] = [Watt] * [second] \quad (12)$$

For all experiments the exposure time was constantly set to 1000 ms, the power of 1,9 W then equals 1,9 mJ; 1,5 W = 1,5 mJ, etc.

Upon leaving the laser, the laser beam normally has a circular or slightly ellipsoidal shape. Therefore it must have been shaped using various lenses to achieve the desired thin light sheet needed for PIV. Following lenses were used for the measurement (in order from laser in direction of water) **(Figure 12)**:

- Plano-concave $f = -50$
- Plano-convex $f = +50$
- Plano-cylindrical $f = -25$

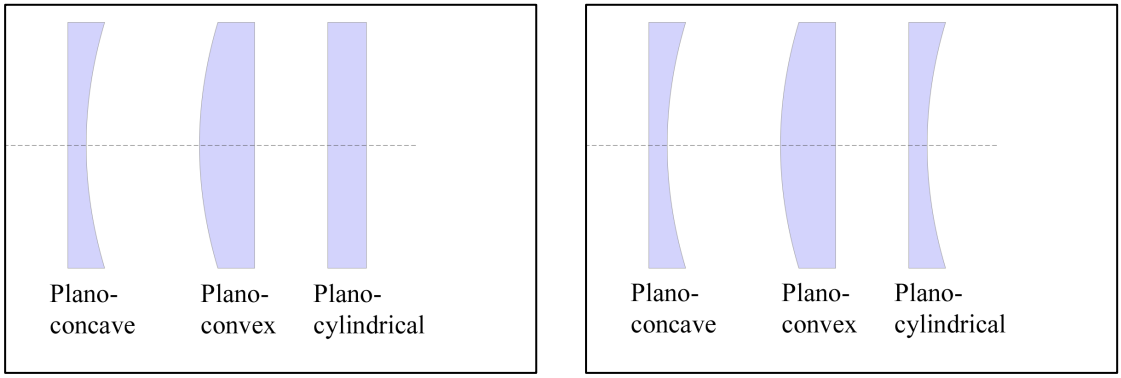

Figure 12 - Top view (left) and a side view of the lenses configuration

Subsequent table shows how the laser sheet height and thickness varies with the distance from the light source and the different intensity of the beam source. Sheet height and thickness were measured right after entering the water (left when watched by the camera, first value), in front of the camera (second value) and again before leaving the water (third value). For a higher precision, its thickness was measured under a constant angle of 60 degrees (See **Figure 13**).

Table 5 - Laser sheet dimensions

Laser power [W; mJ]	Laser thickness 1 [m]	Laser thickness 2 [m]	Laser thickness 3 [m]	Laser height 1 [m]	Laser height 2 [m]	Laser height 3 [m]
0,4	$3{,}2 * 10^{-4}$	$4{,}8 * 10^{-4}$	$6{,}4 * 10^{-4}$	$7{,}5 * 10^{-2}$	$8{,}0 * 10^{-2}$	$8{,}3 * 10^{-2}$
1,0	$3{,}2 * 10^{-4}$	$4{,}8 * 10^{-4}$	$8{,}0 * 10^{-4}$	$7{,}5 * 10^{-2}$	$8{,}3 * 10^{-2}$	$8{,}5 * 10^{-2}$
1,5	$3{,}2 * 10^{-4}$	$4{,}8 * 10^{-4}$	$9{,}6 * 10^{-4}$	$8{,}4 * 10^{-2}$	$9{,}5 * 10^{-2}$	$11{,}0 * 10^{-2}$
2,0	$4{,}8 * 10^{-4}$	$6{,}4 * 10^{-4}$	$9{,}6 * 10^{-4}$	$10{,}0 * 10^{-2}$	$11{,}0 * 10^{-2}$	$12{,}0 * 10^{-2}$

Using the measured values, area lit by the laser sheet could be calculated separately for all three cross-sections. In the next step, volume of the laser sheet in water could be estimated using the mean value of a lit area and the length of the whole measured area (aquarium). **Table 5** shows how the size of the laser sheet varies with the changing intensity of the laser beam.

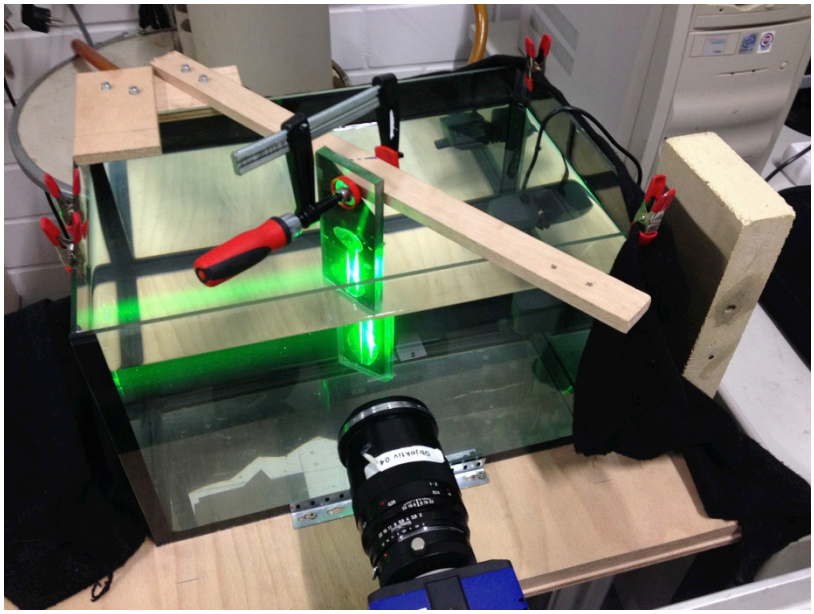

Figure 13 - Measuring the laser sheet

To estimate a number of particles to be seen in front of the camera, a *volume of the AOI* had to be computed. This abbreviation stands for *Area Of Interest*, which is a volume defined by the *laser sheet width* in front of the camera (second column of **Table 5**) and *width and height of camera image at the distance of the laser sheet plane* **(Figure 15).** Its size increases distinctly with the laser intensity (**Figure 14**).

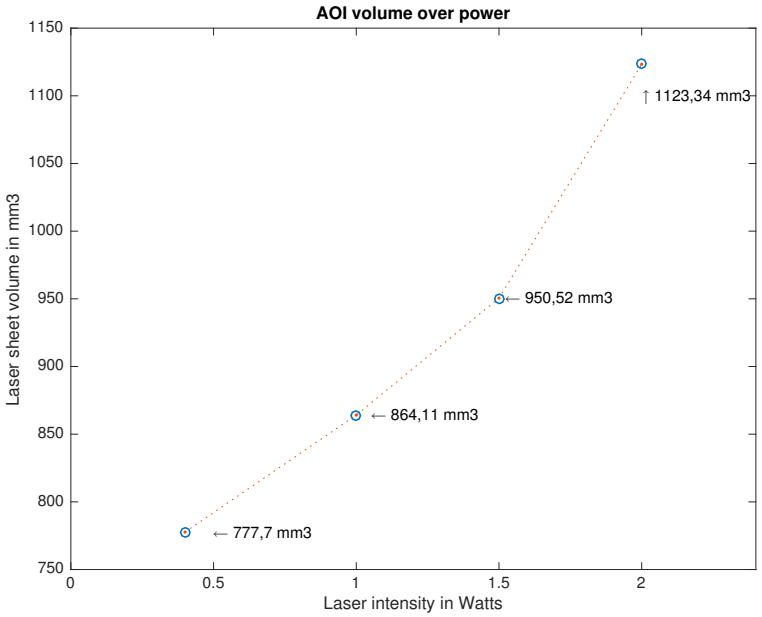

Figure 14 - AOI volume over power for standard AOI (45x36mm)

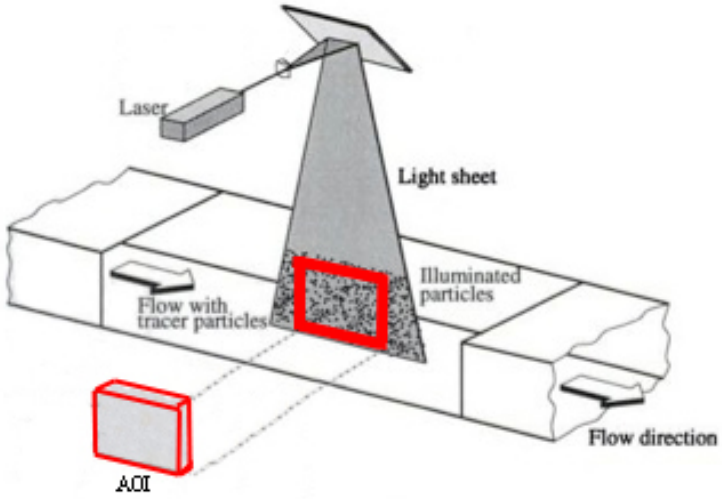

Figure 15 - AOI definition

Note: As stated above, laser power values presented in this work were always measured right at the laser. However, this power is further reduced by lenses, aquarium glass, water and finally by the fact, that the camera is centred only on a part of the laser sheet. Particle images are therefore in the end illuminated by a fraction of the light only. However, there were no means how to measure this value experimentally.

3.3 Seeding Particles

Using a high precision digital weight scale (resolution of 0,001g) a known mass of particles (usually 0,05g) was inserted into the water. With the help of the known

density (provided in the technical specification) and volume of each particle (sphere-like shape), the mass of a single particle could be estimated. In the next step, the total number of particles used could be calculated. If their total number is known, volume of water in the aquarium is known and the volume of the AOI is also known, the expected number of particles in AOI could be calculated.

This value unfortunately differed from the measured one, which was n-times higher. It was therefore necessary to run measurements without any seeding particles to get some data to compare with. Any dust or other dirt might have served as a seeding. Although all necessary precautions were taken to minimize the quantity of foreign elements in the volume, water could have never been completely freed of them. And since the aquarium was , any dirt might have contaminated by air from above. According to Wikipedia, "*the ambient air outside in a typical urban environment contains 35 000 000 particles per cubic meter in the size range 0.5 μm and larger in diameter"* [12]. So their presence could have been significantly influencing the data. To get a reasonable mean value, 30 pictures were taken for the laser power 1500, 1100, 700 and 300 mW. Nevertheless, after the analysis there were only very few particles (1-10) found on these images, which means that the increase of number of particles on the image must have been caused by a different phenomena. It will be further discussed in chapter **Experiments and Results**.

3.4 Camera

Images were taken with *LaVision Imager Pro* high-speed camera with a maximal resolution of 1280 x 1024 pixels. It was controlled by the DaVis software and recorded images were then exported as grayscale TIF files in 8bit.

8bit grayscale image is basically a matrix with 1280 columns and 1024 rows where every cell represents a pixel and contains a value from 0 to 255 (2^8 = 256 values). Zero corresponds to the darkest pixel, 255 to the brightest.

3.5 Analysis Software

To quickly analyse the vast number of images with thousands of particles and extract the sought data, it was necessary to develop an objective analytical method. It was programmed from scrap using Matlab R2015b software, equipped with Image Processing Toolbox v9.3 with an aim to provide namely following data:

- Number of particles
- Mean brightness of a particle

- SNR
- Average particle diameter

The program was for easier handling divided into four subprograms:

- *START_Folder_opener_vX_Y*
- *Particle_counter_vX.Y*
- *Img_histogram_vX.Y*
- *Img_analysis_vX.Y*

3.5.1 START_Folder_opener

START_Folder_opener_vX_Y is based on a program *recurse_subfolders.m* [13] written by a Matlab programmer nicknamed Image Analyst. It allows a fully automatic analysis of vast amount of data if they are stored in a sorted file tree. After choosing a folder with the subfolders with images in a GUI, the program automatically lists them all and opens them respectively. If they include any image files, program runs a function *Particle_counter_vX.Y.* While reaching the end, program opens the next subfolder, etc. Program runs on Windows OS only.

3.5.2 START_Folder_opener_v5_3.m

```
%%%%%%%%%  START_Folder_opener_v5_3.m  %%%%%%%%%%

% Start with a folder and get a list of all subfolders.
% Finds and prints names of all PNG, JPG, and TIF images in
% that folder and all of its subfolders.
clc; clear all; close all;
workspace;  % Make sure the workspace panel is showing.
format longg;
format compact;

% Define a starting folder.
start_path = fullfile(matlabroot, '\toolbox\images\imdemos');
% Ask user to confirm or change.
topLevelFolder = uigetdir(start_path);
if topLevelFolder == 0
    return;
end
% Get list of all subfolders.
allSubFolders = genpath(topLevelFolder);
% Parse into a cell array.
remain = allSubFolders;
listOfFolderNames = {};
while true
    [singleSubFolder, remain] = strtok(remain, ';');
    if isempty(singleSubFolder)
        break;
    end
    listOfFolderNames = [listOfFolderNames singleSubFolder];
end
numberOfFolders = length(listOfFolderNames)
```

```
% Process all image files in those folders.
for k = 1 : numberOfFolders
    % Get this folder and print it out.
    thisFolder = listOfFolderNames{k};
    fprintf('Processing folder %s\n', thisFolder);
    % Get TIF files.
    filePattern = sprintf('%s/*.tif', thisFolder);
    baseFileNames = dir(filePattern);
%     % Get PNG files.
%    filePattern = sprintf('%s/*.png', thisFolder);
%    baseFileNames = dir(filePattern);
%    % Add on TIF files.
%    filePattern = sprintf('%s/*.tif', thisFolder);
%    baseFileNames = [baseFileNames; dir(filePattern)];
%       Add on JPG files.
%    filePattern = sprintf('%s/*.jpg', thisFolder);
%    baseFileNames = [baseFileNames; dir(filePattern)];
    numberOfImageFiles = length(baseFileNames);
    % Now we have a list of all files in this folder.
    if numberOfImageFiles >= 1
        % Go through all those image files.
        [Save_txt_file_as] = Particle_counter_v5_3(numberOfImageFiles,...
            ...thisFolder,baseFileNames)
%        for f = 1 : numberOfImageFiles
%            fullFileName = fullfile(thisFolder, baseFileNames(f).name);
%            fprintf('     Processing image file %s\n', fullFileName);
%          end
    else
        fprintf('     Folder %s has no image files in it.\n', thisFolder);
    end
```

3.5.3 Particle_counter

The basic idea of *Particle_counter_vX.Y* was utilized from the work of Casper et al. [14] As the only input serves the number of images in the folder (DaVis software automatically exports images in the format *B00001.tif*). In the first step program creates an average image from all images in the current set (usually 10-50) by calculating the arithmetic mean for every pixel (see **Figure 16**). This average image is then used in both sub functions as will be explained later. Final results are eventually stored in an automatically created file *Results.txt*.

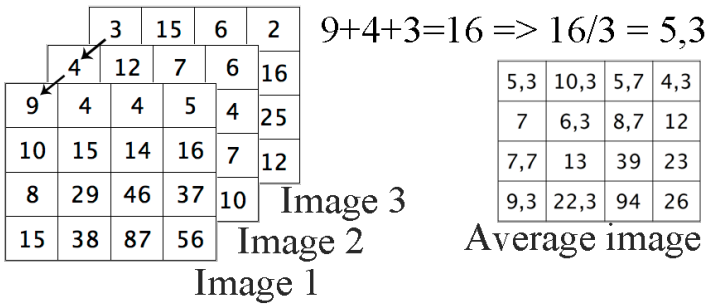

Figure 16 – Arithmetic mean of a pixel and resulting average image. Each box with a number represents a pixel. Pixel`s value corresponds to the intensity captured by the pixel.

3.5.4 Particle_counter_v5_3.m

```
%%%%%%%%%  Particle_counter_v5_3.m  %%%%%%%%%%

%close all; clear all; clc
function [Save_txt_file_as] = Particle_counter_v5_3(p,Program_path,...
    ...baseFileNames)
tic; % Start the timer
format compact;

c=0;
Save_to_path = Program_path(1:end);
Save_txt_file_as = 'Results_v5.txt';
Img_Matrix = zeros(1024, 1280);
Dummy_Matrix1 = zeros(1024, 1280);
Dummy_Matrix2 = zeros(1024, 1280);

% Collect data for average image
for i=1:p;
            c=c+1;
            %display(i)
            File_name = [Program_path,'\',baseFileNames(i).name]
            %['B0000' num2str(i) '.tif']

            Dummy_Matrix1 = imread(File_name);
            Dummy_Matrix2 = double(Dummy_Matrix1);
            Img_Matrix = Img_Matrix + Dummy_Matrix2;
            Dummy_Matrix1 = zeros(1024, 1280);
end

% Generate average image
AVG_img = (1/p)*Img_Matrix;
% Save average image as a different format in order to be able to
% subtract it from images in next steps
AVG_img_2 = AVG_img / 255;
AVG_img_2 = im2uint8(AVG_img_2);
% Export average image so it can be used in Img_histogram and ...
% ...Img_analysis program
setappdata(0,'AVG_img_2',AVG_img_2);

% Loop through all images in set and deliver a histogram data using
% Img_histogram_vX.Y.m
n=0;
for i=1:p;
            n=n+1;
            display(i);
            File_name = [Program_path,'\',baseFileNames(i).name];
            [Sum_of_particles_hist_15_temp,...
                Sum_of_particles_hist_31_temp,...
                Sum_of_particles_hist_47_temp,...
                Sum_of_particles_hist_63_temp,...
                Sum_of_particles_hist_79_temp,...
                Sum_of_particles_hist_95_temp,...
                Sum_of_particles_hist_111_temp,...
                Sum_of_particles_hist_127_temp,...
                Sum_of_particles_hist_143_temp,...
                Sum_of_particles_hist_159_temp,...
                Sum_of_particles_hist_175_temp,...
                Sum_of_particles_hist_191_temp,...
                Sum_of_particles_hist_207_temp,...
                Sum_of_particles_hist_223_temp,...
                Sum_of_particles_hist_239_temp,...
                Sum_of_particles_hist_250_temp]...
                = Img_histogram_v5_3(i, File_name);
            Sum_of_particles_hist_15(n) = Sum_of_particles_hist_15_temp;
            Sum_of_particles_hist_31(n) = Sum_of_particles_hist_31_temp;
            Sum_of_particles_hist_47(n) = Sum_of_particles_hist_47_temp;
```

```
            Sum_of_particles_hist_63(n) = Sum_of_particles_hist_63_temp;
            Sum_of_particles_hist_79(n) = Sum_of_particles_hist_79_temp;
            Sum_of_particles_hist_95(n) = Sum_of_particles_hist_95_temp;
            Sum_of_particles_hist_111(n) = Sum_of_particles_hist_111_temp;
            Sum_of_particles_hist_127(n) = Sum_of_particles_hist_127_temp;
            Sum_of_particles_hist_143(n) = Sum_of_particles_hist_143_temp;
            Sum_of_particles_hist_159(n) = Sum_of_particles_hist_159_temp;
            Sum_of_particles_hist_175(n) = Sum_of_particles_hist_175_temp;
            Sum_of_particles_hist_191(n) = Sum_of_particles_hist_191_temp;
            Sum_of_particles_hist_207(n) = Sum_of_particles_hist_207_temp;
            Sum_of_particles_hist_223(n) = Sum_of_particles_hist_223_temp;
            Sum_of_particles_hist_239(n) = Sum_of_particles_hist_239_temp;
            Sum_of_particles_hist_250(n) = Sum_of_particles_hist_250_temp;
            Save_as_name{n} = File_name;
end

% Calculate 'median value' at each treshold and print to txt file
% (Note: “omitnan” = omit if not a number)
medianSum_of_particles_hist_15 = ...
    median(Sum_of_particles_hist_15,'omitnan');
medianSum_of_particles_hist_31 = ...
median(Sum_of_particles_hist_31,'omitnan');
medianSum_of_particles_hist_47 = ...
median(Sum_of_particles_hist_47,'omitnan');
medianSum_of_particles_hist_63 = ...
median(Sum_of_particles_hist_63,'omitnan');
medianSum_of_particles_hist_79 = ...
median(Sum_of_particles_hist_79,'omitnan');
medianSum_of_particles_hist_95 = ...
median(Sum_of_particles_hist_95,'omitnan');
medianSum_of_particles_hist_111 = ...
median(Sum_of_particles_hist_111,'omitnan');
medianSum_of_particles_hist_127 = ...
median(Sum_of_particles_hist_127,'omitnan');
medianSum_of_particles_hist_143 = ...
median(Sum_of_particles_hist_143,'omitnan');
medianSum_of_particles_hist_159 = ...
median(Sum_of_particles_hist_159,'omitnan');
medianSum_of_particles_hist_175 = ...
median(Sum_of_particles_hist_175,'omitnan');
medianSum_of_particles_hist_191 = ...
median(Sum_of_particles_hist_191,'omitnan');
medianSum_of_particles_hist_207 = ...
median(Sum_of_particles_hist_207,'omitnan');
medianSum_of_particles_hist_223 = ...
median(Sum_of_particles_hist_223,'omitnan');
medianSum_of_particles_hist_239 = ...
median(Sum_of_particles_hist_239,'omitnan');
medianSum_of_particles_hist_250 = ...
median(Sum_of_particles_hist_250,'omitnan');

% From data above calculate how many particles are in each group
Sum_of_particles_in_group1  = medianSum_of_particles_hist_15 -  ...
    medianSum_of_particles_hist_31;
Sum_of_particles_in_group2  = medianSum_of_particles_hist_31 -  ...
    medianSum_of_particles_hist_47;
Sum_of_particles_in_group3  = medianSum_of_particles_hist_47 -  ...
    medianSum_of_particles_hist_63;
Sum_of_particles_in_group4  = medianSum_of_particles_hist_63 -  ...
    medianSum_of_particles_hist_79;
Sum_of_particles_in_group5  = medianSum_of_particles_hist_79 -  ...
    medianSum_of_particles_hist_95;
Sum_of_particles_in_group6  = medianSum_of_particles_hist_95 -  ...
    medianSum_of_particles_hist_111;
Sum_of_particles_in_group7  = medianSum_of_particles_hist_111 - ...
    medianSum_of_particles_hist_127;
Sum_of_particles_in_group8  = medianSum_of_particles_hist_127 - ...
    medianSum_of_particles_hist_143;
Sum_of_particles_in_group9  = medianSum_of_particles_hist_143 - ...
```

```
    medianSum_of_particles_hist_159;
Sum_of_particles_in_group10 = medianSum_of_particles_hist_159 - ...
    medianSum_of_particles_hist_175;
Sum_of_particles_in_group11 = medianSum_of_particles_hist_175 - ...
    medianSum_of_particles_hist_191;
Sum_of_particles_in_group12 = medianSum_of_particles_hist_191 - ...
    medianSum_of_particles_hist_207;
Sum_of_particles_in_group13 = medianSum_of_particles_hist_207 - ...
    medianSum_of_particles_hist_223;
Sum_of_particles_in_group14 = medianSum_of_particles_hist_223 - ...
    medianSum_of_particles_hist_239;
Sum_of_particles_in_group15 = medianSum_of_particles_hist_239 - ...
    medianSum_of_particles_hist_250;
Sum_of_particles_in_group16 = medianSum_of_particles_hist_250;
% Sent results to Img_analysis_vX.Y.m
setappdata(0,'Sum_of_particles_in_group1',Sum_of_particles_in_group1);
setappdata(0,'Sum_of_particles_in_group2',Sum_of_particles_in_group2);
setappdata(0,'Sum_of_particles_in_group3',Sum_of_particles_in_group3);
setappdata(0,'Sum_of_particles_in_group4',Sum_of_particles_in_group4);
setappdata(0,'Sum_of_particles_in_group5',Sum_of_particles_in_group5);
setappdata(0,'Sum_of_particles_in_group6',Sum_of_particles_in_group6);
setappdata(0,'Sum_of_particles_in_group7',Sum_of_particles_in_group7);
setappdata(0,'Sum_of_particles_in_group8',Sum_of_particles_in_group8);
setappdata(0,'Sum_of_particles_in_group9',Sum_of_particles_in_group9);
setappdata(0,'Sum_of_particles_in_group10',Sum_of_particles_in_group10);
setappdata(0,'Sum_of_particles_in_group11',Sum_of_particles_in_group11);
setappdata(0,'Sum_of_particles_in_group12',Sum_of_particles_in_group12);
setappdata(0,'Sum_of_particles_in_group13',Sum_of_particles_in_group13);
setappdata(0,'Sum_of_particles_in_group14',Sum_of_particles_in_group14);
setappdata(0,'Sum_of_particles_in_group15',Sum_of_particles_in_group15);
setappdata(0,'Sum_of_particles_in_group16',Sum_of_particles_in_group16);


% Loop through the images once again and analyze them using
% Img_analysis_vX.Y.m
n=0;
for i=1:p;
            n=n+1;
            display(i);
            File_name = [Program_path,'\',baseFileNames(i).name];
            [Sum_of_particles_temp, Mean_brightness_temp, SNR_temp, ...
                Avg_partcl_diameter_in_mikrons_temp]...
                = Img_analysis_v5_3(i, File_name);
            Sum_of_particles(n) = Sum_of_particles_temp;
            Save_as_name{n} = File_name;
            Mean_brightness(n) = Mean_brightness_temp;
            SNR(n) = SNR_temp;
            %MostFrequent(n) = MostFrequent_temp;
            Avg_partcl_diameter_in_mikrons(n) = ...
                Avg_partcl_diameter_in_mikrons_temp;
            %Saturated(n) = Saturated_pixels_temp;
end

% Stop the timer
wtime = toc;

% Print results of 'Particle_counter.m' to txt file
t = datetime('now','TimeZone','local','Format','d-MMM-y HH:mm');
DateString = datestr(t);
% a+ will add new results into the existing Results.txt file
fid = fopen([Save_txt_file_as] ,'a+');
fprintf(fid, '%s\r', Program_path);
fprintf(fid, 'Datestamp %s\r', DateString');
fprintf(fid, 'Elapsed time = %.0f seconds\r', wtime );
fprintf(fid, 'FilterIndex = 15 \r\r');
fprintf(fid,  'VARIABLES = "Name", "Amount of particles",'...
    '"Mean brightness", "SNR", "Avg particle diameter in mikrons^2"\r');
```

```
% Compute 'median value' and print to txt file
medianSum_of_particles = median(Sum_of_particles,'omitnan');
medianMean_brightness = median(Mean_brightness,'omitnan');
medianSNR = median(SNR,'omitnan');
medianAvg_partcl_diameter_in_mikrons = ...
    median(Avg_partcl_diameter_in_mikrons,'omitnan');

fprintf(fid, 'Median values\r');
fprintf(fid, 'Median, %.0f, %.2f, %.5f, %.2f\r', ...
    medianSum_of_particles, medianMean_brightness, medianSNR, ...
    medianAvg_partcl_diameter_in_mikrons);

% Compute 'standard deviation' and print to txt file
stddevSum_of_particles = std(Sum_of_particles,'omitnan');
stddevMean_brightness = std(Mean_brightness,'omitnan');
stddevSNR = std(SNR,'omitnan');
stddevAvg_partcl_diameter_in_mikrons = ...
    std(Avg_partcl_diameter_in_mikrons,'omitnan');
fprintf(fid, 'Standard deviation\r');
fprintf(fid, 'Stddev, %.0f, %.2f, %.5f, %.2f\r', ...
    stddevSum_of_particles, stddevMean_brightness, stddevSNR, ...
    stddevAvg_partcl_diameter_in_mikrons);

% Print results of 'Img_histogram.m' to txt file
fprintf(fid, 'Histogram tresholds\r');
fprintf(fid, 'Tresholds, 15, 31, 47, 63, 79, 95, 111, 127, 143, 159,'...
    '175, 195, 215, 235, 250\r');

fprintf(fid, 'Histogram data\r');
fprintf(fid, 'Histogram, %.0f, %.0f, %.0f, %.0f, %.0f, %.0f, %.0f,'...
    '%.0f, %.0f, %.0f, %.0f, %.0f, %.0f, %.0f, %.0f, %.0f\r',...
    Sum_of_particles_in_group1, Sum_of_particles_in_group2, ...
    Sum_of_particles_in_group3, Sum_of_particles_in_group4, ...
    Sum_of_particles_in_group5, Sum_of_particles_in_group6, ...
    Sum_of_particles_in_group7, Sum_of_particles_in_group8, ...
    Sum_of_particles_in_group9, Sum_of_particles_in_group10, ...
    Sum_of_particles_in_group11, Sum_of_particles_in_group12, ...
    Sum_of_particles_in_group13, Sum_of_particles_in_group14, ...
    Sum_of_particles_in_group15, Sum_of_particles_in_group16);
fprintf(fid, 'Mean particle brightness =, %.2f\r\r\r\r\r', ...
    medianMean_brightness);

% Close printed txt file
fclose(fid);
display('DONE - STARTER PROGRAM end');
```

3.5.5 Img_histogram

As the name suggest, *Img_histogram_vX.Y* delivers histogram data, i.e. number of particles with certain light intensity, of the image. It uses the average image from the previous step, which is then subtracted from the examined image in order to reduce the background noise. The result is then called Filtered image.

The backbone of the analysis is Matlab function *Image contours (imcontour)* that draws a contour plot of the grayscale image. Contours are lines connecting pixels with a certain brightness, which can be chosen by the user. Every particle image basically looks as a hill and the engine draws a circle-like-line around it. Imcontour then generates a long matrix where coordinates of all contour lines are stored. In order

to count the particles suffices to count the number of appearances of the chosen intensity value in the matrix. (Note: *imcontour* function requires Image Processing Toolbox installed in order to work).

In the beginning it was relatively hard to find the right value, which would find even the faintest particle, but which would also omit background noise. Since the average background noise intensity oscillated around the value of 6-9, as a reasonable value was chosen 15.

There are more ways how to count particles on an image. Quite often Matlab function *regionprops* is used. It can measure various properties, such as area, location of the centroid, radius, etc. for chosen image regions. But it requires the image to be black and white, which has a great disadvantage of loosing the "texture" of the image. Unlike grayscale image, black and white image has only completely black, or completely white regions; it cannot show any shades of grey.

Figure 17 shows left upper part of the image (with slightly increased brightness to make the particles more visible) recorded by the camera and the same image after analysis in Matlab. Imcontour is capable of finding the defined value (e.g. 15) although it is not actually depicted by any pixel – it wisely works on a sub pixel level. From this point of view it was therefore sufficient to work with 8bit images only, although the camera was capable to record even in 16bit. Higher bit rate would more precisely depict the location of the contour, but also cause larger images and longer analysis.

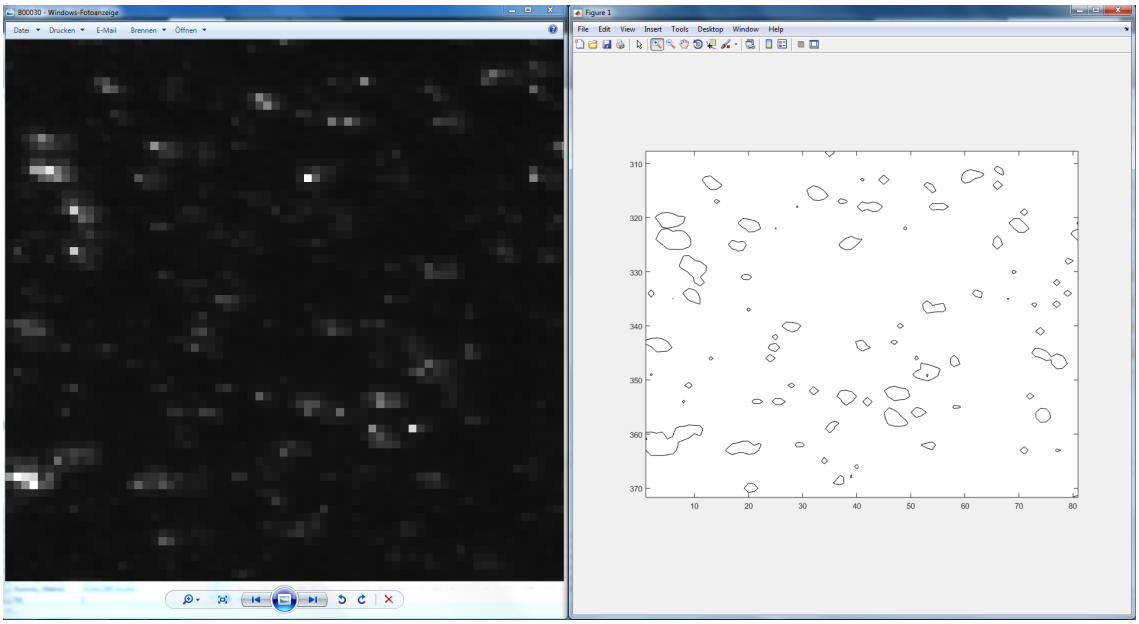

Figure 17 - Image contours – raw and analysed left upper corner of an image

In order to determine the 16-step histogram of the image, contours are searched for 15 values from 15 to 250 (15, 31, 47, 63, 79, 95, 111, … 250). The results are then exported to the *Img_analysis_vX_Y*.

3.5.6 Img_histogram_v5_3.m

```
%%%%%%%%%  Img_histogram_v5_3.m  %%%%%%%%%%

function [Sum_of_particles_hist_15, Sum_of_particles_hist_31, ...
     Sum_of_particles_hist_47, Sum_of_particles_hist_63, ...
     Sum_of_particles_hist_79, Sum_of_particles_hist_95, ...
     Sum_of_particles_hist_111, Sum_of_particles_hist_127, ...
     Sum_of_particles_hist_143, Sum_of_particles_hist_159, ...
     Sum_of_particles_hist_175, Sum_of_particles_hist_191, ...
     Sum_of_particles_hist_207, Sum_of_particles_hist_223, ...
     Sum_of_particles_hist_239, Sum_of_particles_hist_250] = ...
     Img_histogram_v5_3(v, File_name)

% Read image
File_name = imread(File_name);

% Get average image calculated by START_Particle_counter
AVG_img_2 = getappdata(0,'AVG_img_2');

% Subtract image from average image to reduce background noise
Filtered_img = imsubtract(File_name,AVG_img_2);

% Draw image contours for following thresholds:
% 15,31,47,63,79,95,111,127,143,159,175,195,215,235,250
v1 = 15;
        % Input parameters for the image contour (least value)
        filter_index0 = v1;
        filter_index1 = v1;     % dtto (max value)
        [C] = imcontour(Filtered_img, [filter_index0 filter_index1],'ok');
        % Count the sum of particles
        Sum_of_particles_hist_15 = (sum(C(:) == filter_index0));

v2 = 31;
        filter_index0 = v2;
        filter_index1 = v2;
        [C] = imcontour(Filtered_img, [filter_index0 filter_index1],'ok');
        % Count the sum of particles
        Sum_of_particles_hist_31 = (sum(C(:) == filter_index0));

v3 = 47;
        filter_index0 = v3;
        filter_index1 = v3;
        [C] = imcontour(Filtered_img, [filter_index0 filter_index1],'ok');
        % Count the sum of particles
        Sum_of_particles_hist_47 = (sum(C(:) == filter_index0));

v4 = 63;
        filter_index0 = v4;
        filter_index1 = v4;
        [C] = imcontour(Filtered_img, [filter_index0 filter_index1],'ok');
        % Count the sum of particles
        Sum_of_particles_hist_63 = (sum(C(:) == filter_index0));

v5 = 79;
        filter_index0 = v5;
        filter_index1 = v5;
        [C] = imcontour(Filtered_img, [filter_index0 filter_index1],'ok');
        % Count the sum of particles
```

```
        Sum_of_particles_hist_79 = (sum(C(:) == filter_index0));

v6 = 95;
        filter_index0 = v6;
        filter_index1 = v6;
        [C] = imcontour(Filtered_img, [filter_index0 filter_index1],'ok');
        % Count the sum of particles
        Sum_of_particles_hist_95 = (sum(C(:) == filter_index0));

v7 = 111;
        filter_index0 = v7;
        filter_index1 = v7;
        [C] = imcontour(Filtered_img, [filter_index0 filter_index1],'ok');
        % Count the sum of particles
        Sum_of_particles_hist_111 = (sum(C(:) == filter_index0));

v8 = 127;
        filter_index0 = v8;
        filter_index1 = v8;
        [C] = imcontour(Filtered_img, [filter_index0 filter_index1],'ok');
        % Count the sum of particles
        Sum_of_particles_hist_127 = (sum(C(:) == filter_index0));

v9 = 143;
        filter_index0 = v9;
        filter_index1 = v9;
        [C] = imcontour(Filtered_img, [filter_index0 filter_index1],'ok');
        % Count the sum of particles
        Sum_of_particles_hist_143 = (sum(C(:) == filter_index0));
v10 = 159;
        filter_index0 = v10;
        filter_index1 = v10;
        [C] = imcontour(Filtered_img, [filter_index0 filter_index1],'ok');
        % Count the sum of particles
        Sum_of_particles_hist_159 = (sum(C(:) == filter_index0));
v11 = 175;
        filter_index0 = v11;
        filter_index1 = v11;
        [C] = imcontour(Filtered_img, [filter_index0 filter_index1],'ok');
        % Count the sum of particles
        Sum_of_particles_hist_175 = (sum(C(:) == filter_index0));
v12 = 191;
        filter_index0 = v12;
        filter_index1 = v12;
        [C] = imcontour(Filtered_img, [filter_index0 filter_index1],'ok');
        % Count the sum of particles
        Sum_of_particles_hist_191 = (sum(C(:) == filter_index0));
v13 = 207;
        filter_index0 = v13;
        filter_index1 = v13;
        [C] = imcontour(Filtered_img, [filter_index0 filter_index1],'ok');
        % Count the sum of particles
        Sum_of_particles_hist_207 = (sum(C(:) == filter_index0));
v14 = 223;
        filter_index0 = v14;
        filter_index1 = v14;
        [C] = imcontour(Filtered_img, [filter_index0 filter_index1],'ok');
        % Count the sum of particles
        Sum_of_particles_hist_223 = (sum(C(:) == filter_index0));
v15 = 239;
        filter_index0 = v15;
        filter_index1 = v15;
        [C] = imcontour(Filtered_img, [filter_index0 filter_index1],'ok');
        % Count the sum of particles
        Sum_of_particles_hist_239 = (sum(C(:) == filter_index0));
v16 = 250;
        filter_index0 = v16;
        filter_index1 = v16;
        [C] = imcontour(Filtered_img, [filter_index0 filter_index1],'ok');
```

```
        % Count the sum of particles
        Sum_of_particles_hist_250 = (sum(C(:) == filter_index0));

    % Export v1-v8 so it can be used in Img_analysis program
setappdata(0,'v1',v1);
setappdata(0,'v2',v2);
setappdata(0,'v3',v3);
setappdata(0,'v4',v4);
setappdata(0,'v5',v5);
setappdata(0,'v6',v6);
setappdata(0,'v7',v7);
setappdata(0,'v8',v8);
setappdata(0,'v9',v9);
setappdata(0,'v10',v10);
setappdata(0,'v11',v11);
setappdata(0,'v12',v12);
setappdata(0,'v13',v13);
setappdata(0,'v14',v14);
setappdata(0,'v15',v15);
setappdata(0,'v16',v16);
end
```

3.5.7 Img_analysis

In the first step *Img_analysis_vX_Y* imports the results from the other programs and counts the number of particles for each histogram column. Mean particle brightness is calculated from histogram by literally computing the x-axis coordinate of the histogram centroid (**Figure 18**).

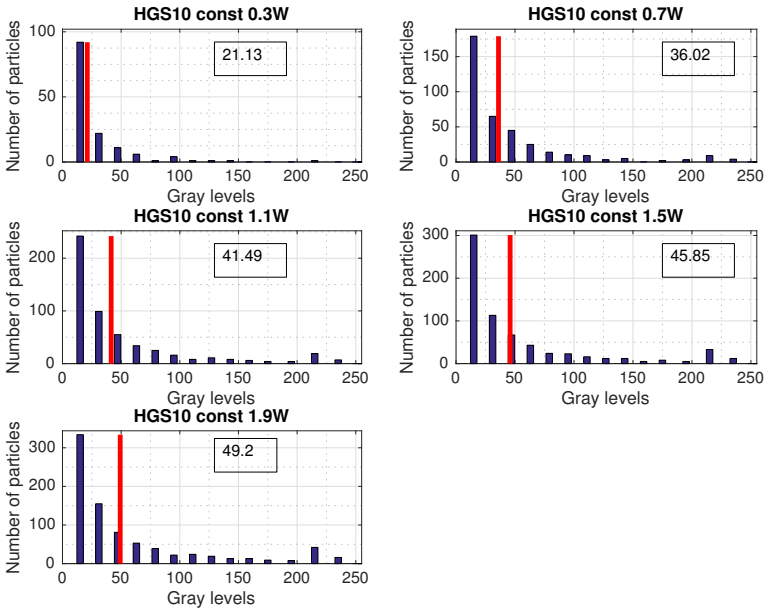

Figure 18 - Histograms of HGS10 for various laser power setting. Computed mean particle brightness shown in red

Signal-to-noise ratio in imaging is defined as the ratio of the average signal value to the standard deviation of the background. [15] Thus it is calculated as:

$$SNR = 10 * \log_{10} \frac{Mean\ particle\ brightness}{Standard\ deviation\ of\ background\ of\ the\ filtered\ image} \quad (13)$$

In the next step diameter of each particle image is calculated using function *regionprops*. As its border serves the contour line set before. The result is for easier understanding then printed in microns. To achieve this, length and height corresponding to a size of a pixel projected on a laser plane at the distance of the laser sheet from the camera had to be found. For the measurements it is 26,69 microns.

3.5.8 Img_analysis_v5_3.m

```
%%%%%%%%%  Img_analysis_v5_3.m  %%%%%%%%%%

function [Sum_of_particles, Mean_brightness, SNR, ...
    Avg_partcl_diameter_in_mikrons_temp] = Img_analysis_v5_3(i, File_name)

% Read image
File_name = imread(File_name);

% Get average image calculated by START_Particle_counter
AVG_img_2 = getappdata(0,'AVG_img_2');

% Subtract image from average image to reduce noise
Filtered_img = imsubtract(File_name,AVG_img_2);

% Convert image to Grayscale
%Gray_img = rgb2gray(Source_img);

%% Draw image contours
filter_index0 = 15;
filter_index1 = 15;
[C,h] = imcontour(Filtered_img, [filter_index0 filter_index1],'ok');

% Count the sum of particles
Sum_of_particles = (sum(C(:) == filter_index0))

%% SNR calculation
% Preparing data (Image data to DOUBLE format)
Filtered_img_noise_SNR = double(Filtered_img(:));
% Standard deviation of brightness values of the Filtered image
Filtered_img_noise_std = std(Filtered_img_noise_SNR(:));

% Area calculation
v1 = getappdata(0,'v1');
v2 = getappdata(0,'v2');
v3 = getappdata(0,'v3');
v4 = getappdata(0,'v4');
v5 = getappdata(0,'v5');
v6 = getappdata(0,'v6');
v7 = getappdata(0,'v7');
v8 = getappdata(0,'v8');
v9 = getappdata(0,'v9');
v10 = getappdata(0,'v10');
v11 = getappdata(0,'v11');
v12 = getappdata(0,'v12');
v13 = getappdata(0,'v13');
v14 = getappdata(0,'v14');
v15 = getappdata(0,'v15');
v16 = getappdata(0,'v16');
```

```
Sum_of_particles_in_group1 = getappdata(0,'Sum_of_particles_in_group1');
Sum_of_particles_in_group2 = getappdata(0,'Sum_of_particles_in_group2');
Sum_of_particles_in_group3 = getappdata(0,'Sum_of_particles_in_group3');
Sum_of_particles_in_group4 = getappdata(0,'Sum_of_particles_in_group4');
Sum_of_particles_in_group5 = getappdata(0,'Sum_of_particles_in_group5');
Sum_of_particles_in_group6 = getappdata(0,'Sum_of_particles_in_group6');
Sum_of_particles_in_group7 = getappdata(0,'Sum_of_particles_in_group7');
Sum_of_particles_in_group8 = getappdata(0,'Sum_of_particles_in_group8');
Sum_of_particles_in_group9 = getappdata(0,'Sum_of_particles_in_group9');
Sum_of_particles_in_group10 = getappdata(0,'Sum_of_particles_in_group10');
Sum_of_particles_in_group11 = getappdata(0,'Sum_of_particles_in_group11');
Sum_of_particles_in_group12 = getappdata(0,'Sum_of_particles_in_group12');
Sum_of_particles_in_group13 = getappdata(0,'Sum_of_particles_in_group13');
Sum_of_particles_in_group14 = getappdata(0,'Sum_of_particles_in_group14');
Sum_of_particles_in_group15 = getappdata(0,'Sum_of_particles_in_group15');
Sum_of_particles_in_group16 = getappdata(0,'Sum_of_particles_in_group16');


% First moment of area
v1_1 = v1;
v2_1 = v2-v1;
v3_1 = v3-v2;
v4_1 = v4-v3;
v5_1 = v5-v4;
v6_1 = v6-v5;
v7_1 = v7-v6;
v8_1 = v8-v7;
v9_1 = v9-v8;
v10_1 = v10-v9;
v11_1 = v11-v10;
v12_1 = v12-v11;
v13_1 = v13-v12;
v14_1 = v14-v13;
v15_1 = v15-v14;
v16_1 = v16-v15;

% Area of histogram
S = (Sum_of_particles_in_group1*v1_1)+(Sum_of_particles_in_group2*v2_1)+...
    (Sum_of_particles_in_group3*v3_1)+(Sum_of_particles_in_group4*v4_1)+...
    (Sum_of_particles_in_group5*v5_1)+(Sum_of_particles_in_group6*v6_1)+...
    (Sum_of_particles_in_group7*v7_1)+(Sum_of_particles_in_group8*v8_1)+...
    (Sum_of_particles_in_group9*v9_1)+(Sum_of_particles_in_group10*v10_1)+...
    (Sum_of_particles_in_group11*v11_1)+...
    (Sum_of_particles_in_group12 *v12_1)+...
    (Sum_of_particles_in_group13 * v13_1)+...
    (Sum_of_particles_in_group14 * v14_1)+...
    (Sum_of_particles_in_group15 * v15_1)+...
    (Sum_of_particles_in_group16 * v16_1);


Sx1  = (Sum_of_particles_in_group1 *  v1_1)  * (v1_1/2);
Sx2  = (Sum_of_particles_in_group2 *  v2_1)  * (v1 + v2_1/2);
Sx3  = (Sum_of_particles_in_group3 *  v3_1)  * (v2 + v3_1/2);
Sx4  = (Sum_of_particles_in_group4 *  v4_1)  * (v3 + v4_1/2);
Sx5  = (Sum_of_particles_in_group5 *  v5_1)  * (v4 + v5_1/2);
Sx6  = (Sum_of_particles_in_group6 *  v6_1)  * (v5 + v6_1/2);
Sx7  = (Sum_of_particles_in_group7 *  v7_1)  * (v6 + v7_1/2);
Sx8  = (Sum_of_particles_in_group8 *  v8_1)  * (v7 + v8_1/2);
Sx9  = (Sum_of_particles_in_group9 *  v9_1)  * (v8 + v9_1/2);
Sx10 = (Sum_of_particles_in_group10 * v10_1) * (v9 + v10_1/2);
Sx11 = (Sum_of_particles_in_group11 * v11_1) * (v10 + v11_1/2);
Sx12 = (Sum_of_particles_in_group12 * v12_1) * (v11 + v12_1/2);
Sx13 = (Sum_of_particles_in_group13 * v13_1) * (v12 + v13_1/2);
Sx14 = (Sum_of_particles_in_group14 * v14_1) * (v13 + v14_1/2);
Sx15 = (Sum_of_particles_in_group15 * v15_1) * (v14 + v15_1/2);
Sx16 = (Sum_of_particles_in_group16 * v16_1) * (v15 + v16_1/2);

% Mean brightness of particles from Histogram
% (calculated as a centroid of the histogram)
Mean_particle_brightness_from_histogram = (Sx1+Sx2+Sx3+Sx4+Sx5+Sx6+...
```

```
    Sx7+Sx8+Sx9+Sx10+Sx11+Sx12+Sx13+Sx14+Sx15+Sx16)/S;

% SNR
SNR = 10*log10(Mean_particle_brightness_from_histogram/...
    Filtered_img_noise_std);

%% Mean brightness of a particle in image
Mean_brightness = Mean_particle_brightness_from_histogram;

%% Calculate area of each particle (particle border is defined as the area
% used for countours function (filter_index0)).
% Img to BW
level_area = filter_index0/255; %to get number btw [0 1] needed for im2bw
Filtered_img_BW = im2bw(Filtered_img, level_area);
% Calculate area of each particle
Area = regionprops(Filtered_img_BW,'Area');
Area_as_cell = struct2cell(Area);
Area_as_matrix = cell2mat(Area_as_cell);
Avg_partcl_size_in_pxls = mean(Area_as_matrix);
Avg_partcl_size_in_pxls_as_circle = sqrt((4*Avg_partcl_size_in_pxls)/pi);
Avg_partcl_diameter_in_mikrons_temp = ...
    Avg_partcl_size_in_pxls_as_circle*29.69;
% 29.69 mikrons = lenght and height of a pixel at
% the distance of a laser sheet
end
```

3.5.9 Image Filtering

As mentioned above, raw images were analysed with Matlab code using average image filtering (see 3.5.2). After the first results had been obtained aroused a concern, if this filtering method was not influencing the results for very bright/large particles such as HGS75 or VEST100. So another three filtering/analysis methods were tried:

- *Mean average of average image* – Filtering by subtracting a mean average of all pixels of an average image from the investigated one
- *Thresh 31* – Raising the threshold of *imcontour* function from 15 to 31. Change of the analysis method itself, standard filtering using average image
- *No filtering* at all

As illustrates **Table 6**, using *Mean average of average image* method subtracts smaller value from an original, so the number of particles illusorily increases same as increases the mean particle brightness. On the other hand the background brightness fluctuates more decreasing the SNR. Higher *threshold of 31* reduces the number of particles found, leaving only the brighter ones, so the mean particle brightness and SNR increases. Use of *no filtering* returns the same number of particles as the standard method, only with a worse mean brightness and SNR.

Table 6 – Comparison of various filtering methods on results for PSP05 (above) and HGS75 (below) at 1,9W

Filtering	No.	Mean particle	SNR	Avg particle

method	**of particles**	**brightness [grayscale]**		**diameter in µm**
Standard	*6339*	*21,61*	*7,06*	*45,93*
Mean Avg	6864	21,64	6,86	46,22
Thresh 31	2323	33,70	8,83	41,98
No filtering	6339	14,68	5,38	45,93
Standard	*1077*	*63,23*	*11,85*	*55,66*
Mean Avg	1138	68,11	11,69	56,6
Thresh 31	699	75,52	12,62	51,48
No filtering	1077	43,79	10,35	55,66

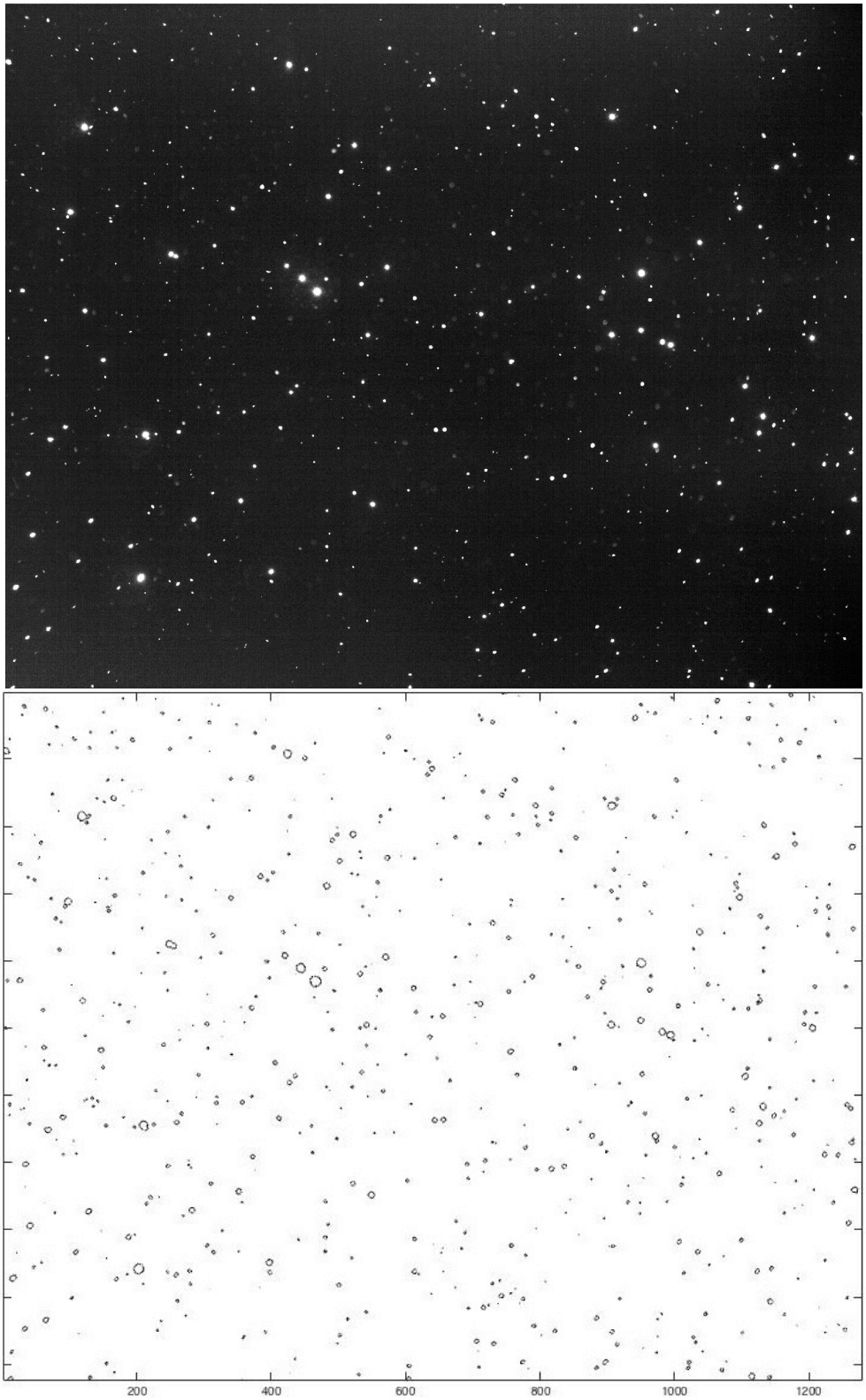

Figure 19 – Example of original and analysed image of VEST100 at 0,7W (Image above had been adjusted for better visibility – brightness +80%, contrast +60%)

4. Experiments and Results

Note: In order to get reliable results, all presented values were computed as a mean average of at least 10 images. For better lucidity four graphs showing a *number of particles*, *mean particle brightness*, *ratio of measured to expected number of particles* and *signal to noise ratio* will always be presented.

4.1 Particles – Real Size and Shape

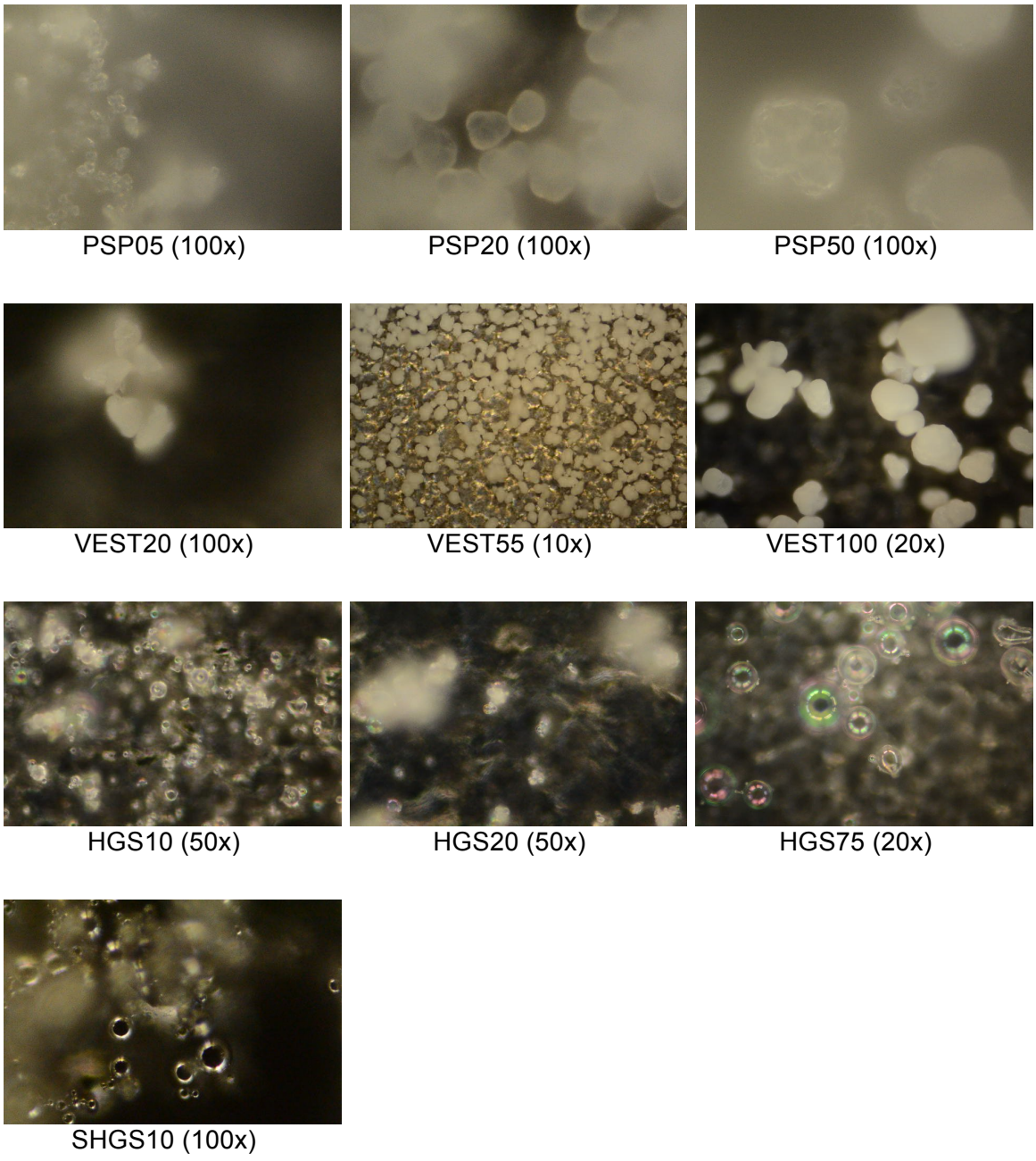

Figure 20 - Images of all sorts taken by the microscope. Magnification in brackets

Particles were studied under a microscope in order to check their real size compared to size in technical specification and also their real shape. That was done in a dry form, i.e. particles were observed as powder, not resolved in water. Magnification was chosen in order to get the best possible image. Unfortunately, it was not always possible to measure the size of more than a few particles **(Table 7**).

Table 7 - All sorts of particles and their measured size

Name	Company	Magnification	Average size in μm (no. of samples measured)	ΔSize [%]
PSP05	Dantec	100x	3,52 (33)	**-29,6 %**
PSP20	Dantec	100x	16,69 (27)	**-16,55 %**
PSP50	Dantec	100x	37,98 (6)	**-24,04 %**
VEST20	LaVision	100x	26,35 (6)	**+31,75 %**
VEST55	LaVision	10x	57,42 (50)	**+4,40 %**
VEST100	LaVision	20x	61,14 (25)	**-38,86 %**
HGS10	Dantec	50x	10,59 (17)	**+5,90 %**
HGS20	LaVision	50x	6,66 (51)	**-69,90 %**
HGS75	LaVision	20x	61,37 (17)	**-18,17 %**
SHGS10	Dantec	100x	6,69 (21)	**-33,10 %**

Results are generally in accordance with reported size (deviations normally occur, manufacturers publish distribution diagrams of particle sizes). Also the used technique of measuring the number of pixels a particle has in diameter influences results by few %. On the other hand HGS20 differ by almost 70% from their published size. Probably it is because of way too small representative amount of particles measured. However, this sort of particles came as a sample from LaVision in a small box. LaVision received it as a sample from a source, which might have differed from the other sources, so it is possible that it was not of the best quality.

4.2 General Particle Properties[2]

4.2.1 Constant Mass of Seeding - 0,05g

Using the experimental setup shown in previous chapter an initial database of images was acquired under following conditions:

- Mass of used seeding 0,05g
- Aperture 2,0
- Shutter speed 1000 ms
- Laser power set in 5 steps from 0,3W to 1,9W

Results, in majority of cases count as averages of more individual measurements, can be seen on **Figure 21**. On the upper left chart (Number of particles) are values significantly spread, so for better recognition of the low-values are they again shown enlarged on **Figure 22**. Red vertical lines show the standard deviation.

As can be seen on the chart, the visible number of particles increases with an increasing laser power, although the density of seeding remains the same. One reason is a widening of a laser sheet itself, but it also suggest that the scattered light might illuminate additionally and in larger scale those particles not directly within a laser plane. This is also probably the reason why the ration between measured and expected number of particles is so high. Since always the same mass of seeding powder was used, number of particles cannot be really compared (much larger or just much denser particles are inevitably represented by fewer pieces). But regardless of this inequality, the number of particles of VEST20 (light blue) was throughout the experiment surprisingly high. It was constantly by one third higher than the number of HGS20 (green) and even more than two times (!) higher than of PSP20 (purple), although it is made from the same or very similar material so it was expected to have very similar density and thus there should be a similar number of particles visible. As can be seen on the right upper chart, VEST20 scatters approximately the same amount of incident light per particle, but since there are n-times more visible particles per volume when using the same laser power, the overall image is much brighter. SNR for VEST20 was the lowest of all measured in this experiment, which only confirms the theory of generally better scattering ability.

[2] Note: Mean particle brightness and SNR`s charts are (with one exception) always shown with a fixed dimensions.

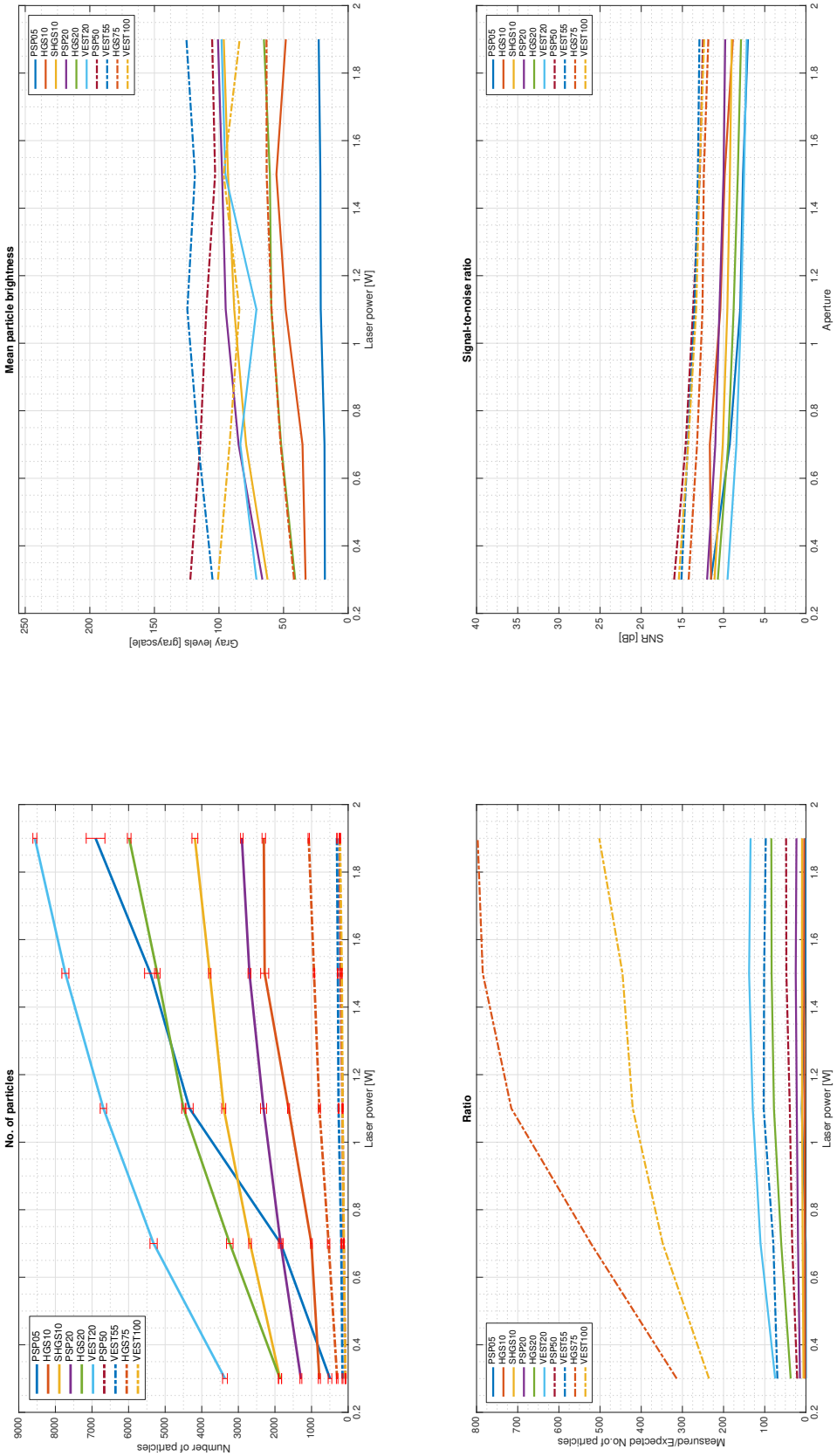

Figure 21 - 0,05g; 1,9W

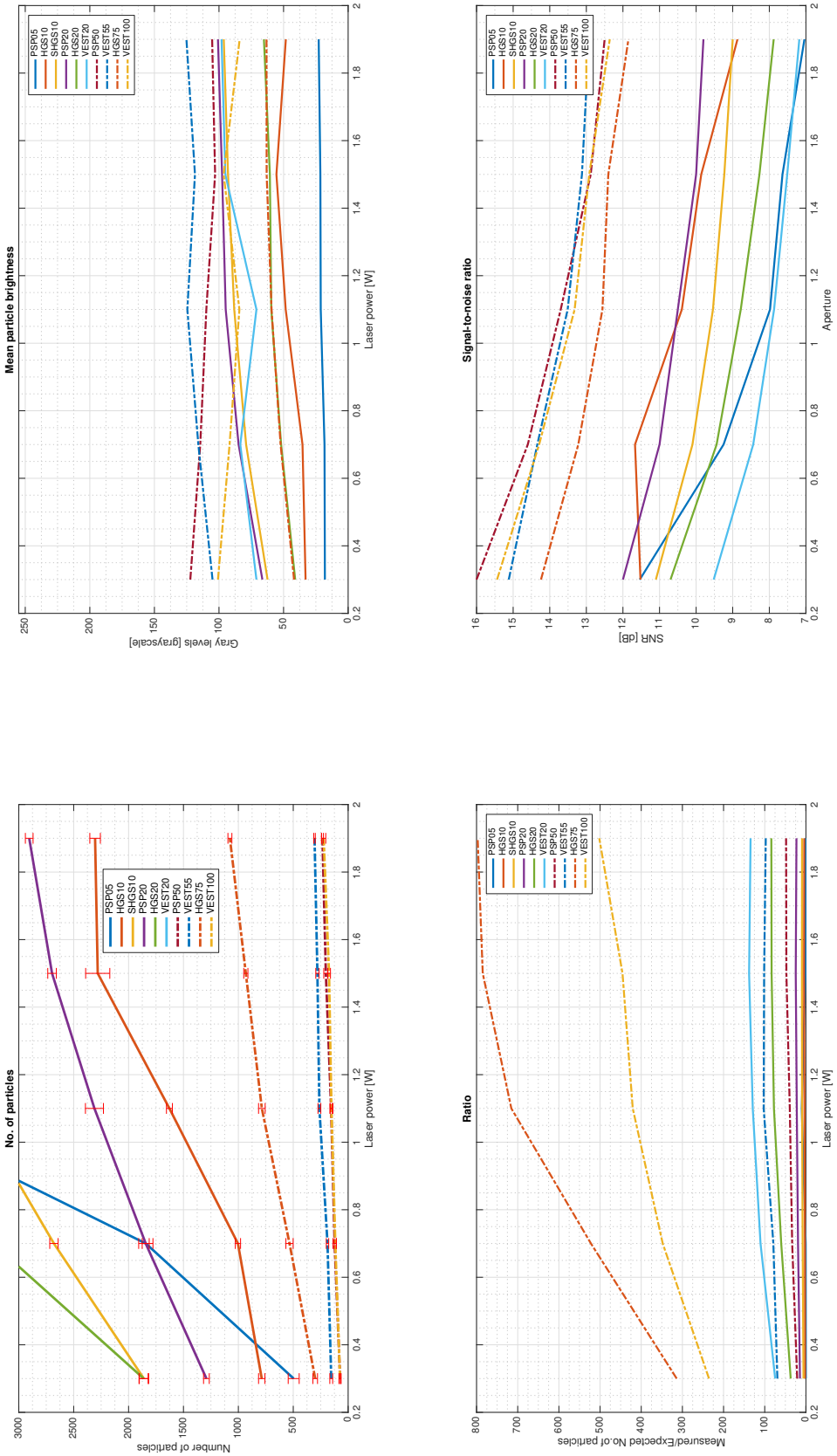

Figure 22 - 0,05g; 1,9W; Lower part only

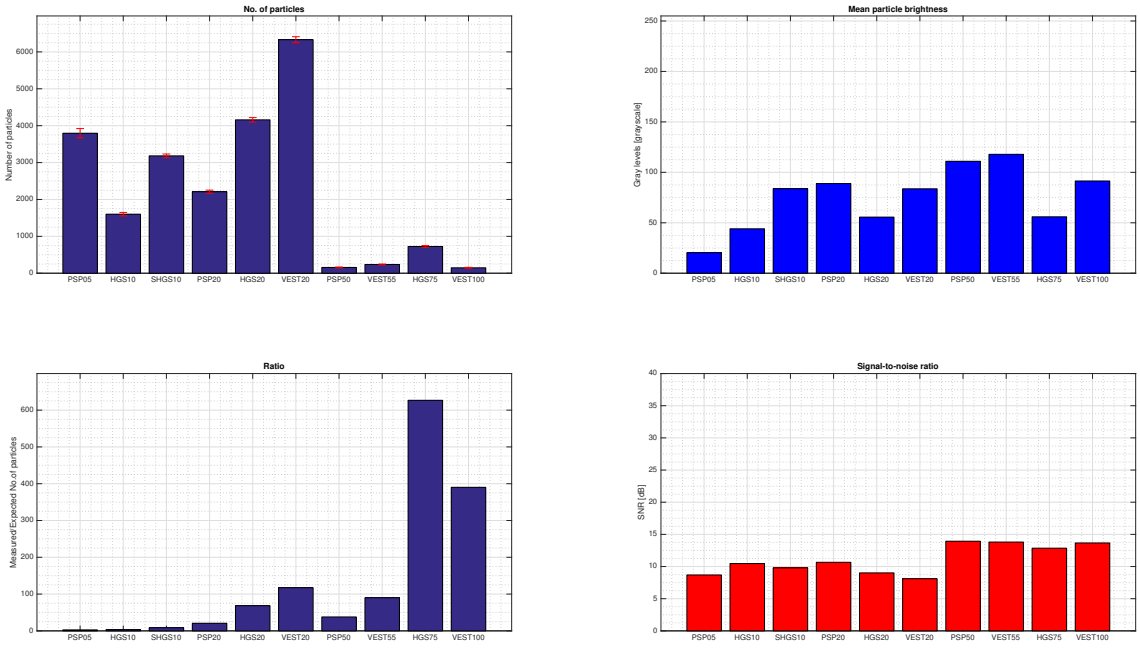

Figure 23 - Comparison of all particle sorts, concentration constantly 0,05g; Values shown are mean averages for all laser power settings

Mean particle brightness of all measured sorts can be further compared on the overview **(Figure 23)**. Particles can be divided, according to their mean brightness, into following groups from highest to lowest brightness (for 0,05g):

1. VEST55, PSP50
2. PSP20, VEST20, SHGS10, VEST100
3. HGS20, HGS75
4. HGS10
5. PSP05

The groups are in general quite consistent with expectations. On the other hand there is a question why VEST100 and HGS75`s brightnesses are so low. This question will be answered in the following chapters.

4.2.2 Constant Number of Particles

Preceding results show huge differences of number of particles between very large and very small particles. As mentioned above it is caused by the fact, that a constant mass of seeding was used. It means, for example, that the concentration of particles bigger than 50 microns was of few orders lower than of small ones. So the idea was to approach the problem from a different side by using constant number of particles for all sorts. But due to a variety of used seeding it was impossible to find one constant number for all sizes, since it lead to a problem of masses that were out of scale –

far bellow the threshold of used digital weight, or far above. Too densely seeded fluid also becomes opaque and study of this behaviour was not a goal of this particular experiment.

Particles were thus divided into three groups and for each one a desired quantity to be placed into the aquarium was set as shown in **Table 8**:

Table 8 - Groups for experiment with a constant number of particles

Number in total	**Name**	**Pieces in AOI (at 1,9W)**
50.000.000	PSP05	2680
5.000.000	HGS10, SHGS10, PSP20, HGS20, VEST20	268
50.000	PSP50, VEST55, HGS75, VEST100	2,68

Volume of the AOI was known, so it was again possible to calculate the expected number of particles in AOI.

On the following **Figures 24-29** can be seen the results:

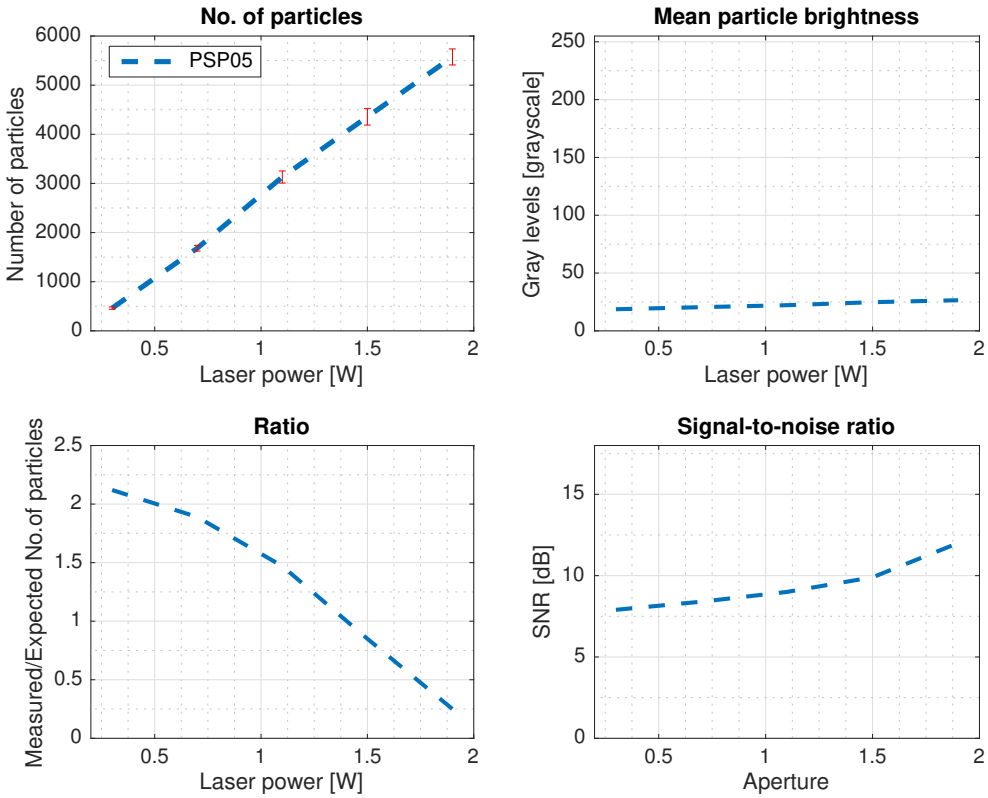

Figure 24 - 50.000.000 of particles in the volume (PSP05)

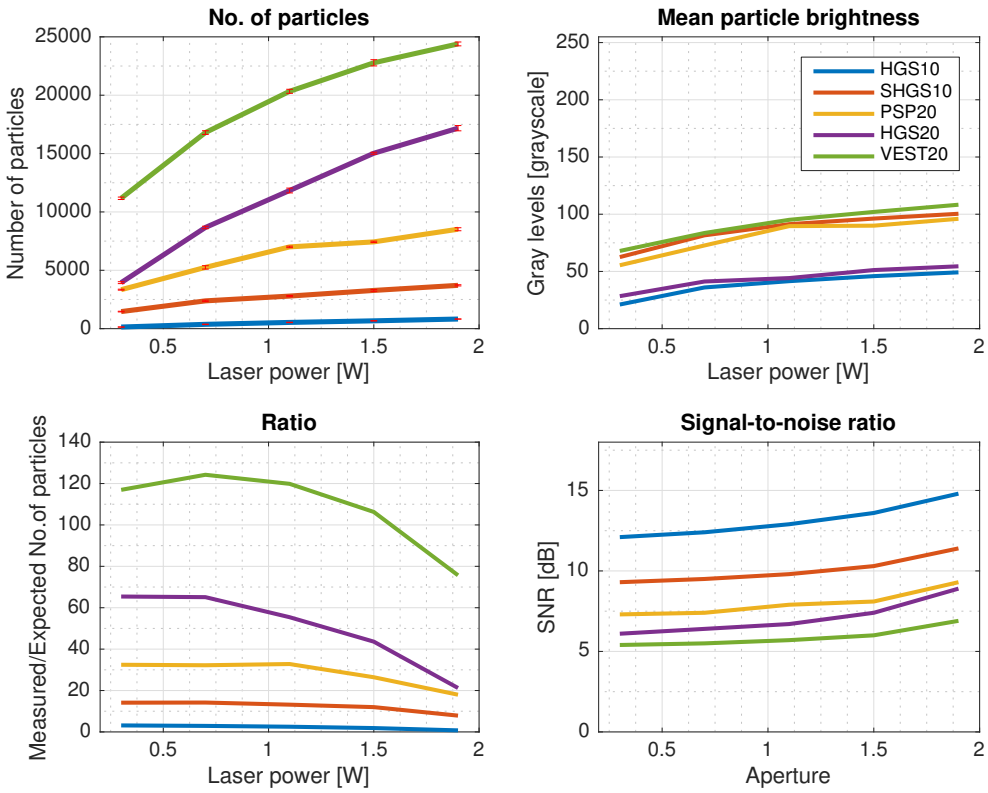

Figure 25 - 5.000.000 of particles in the volume (HGS10, SHGS10, PSP20, HGS20, VEST20)

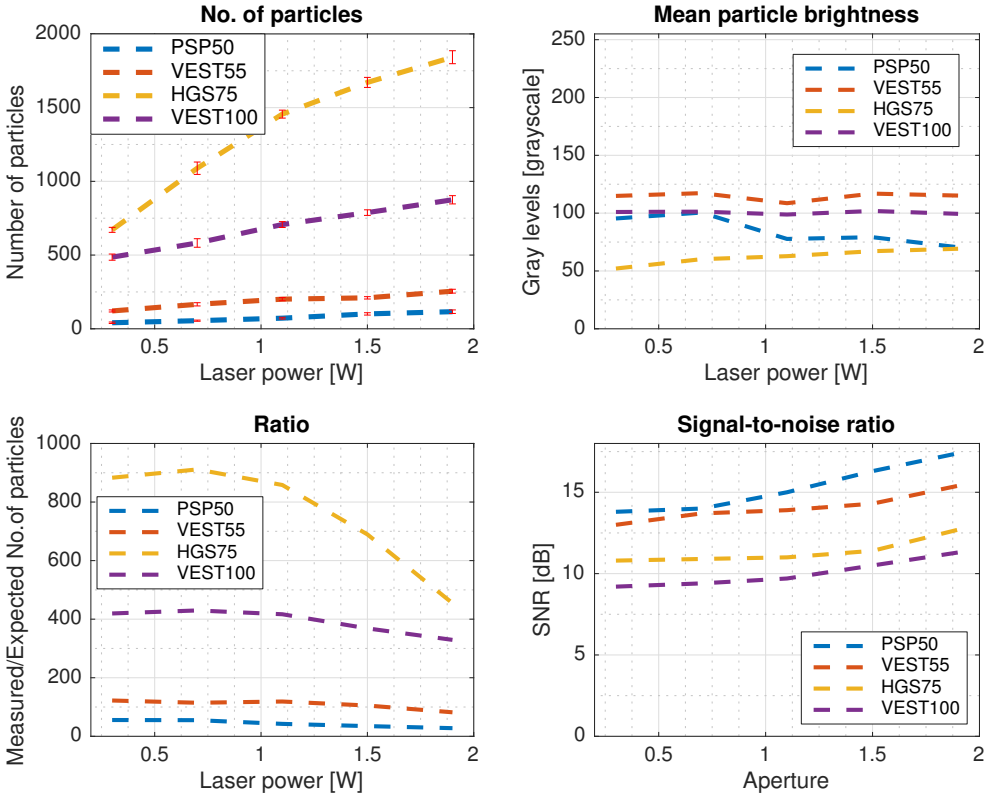

Figure 26 - 50.000 of particles in the volume (PSP50, VEST55, HGS75, VEST100)

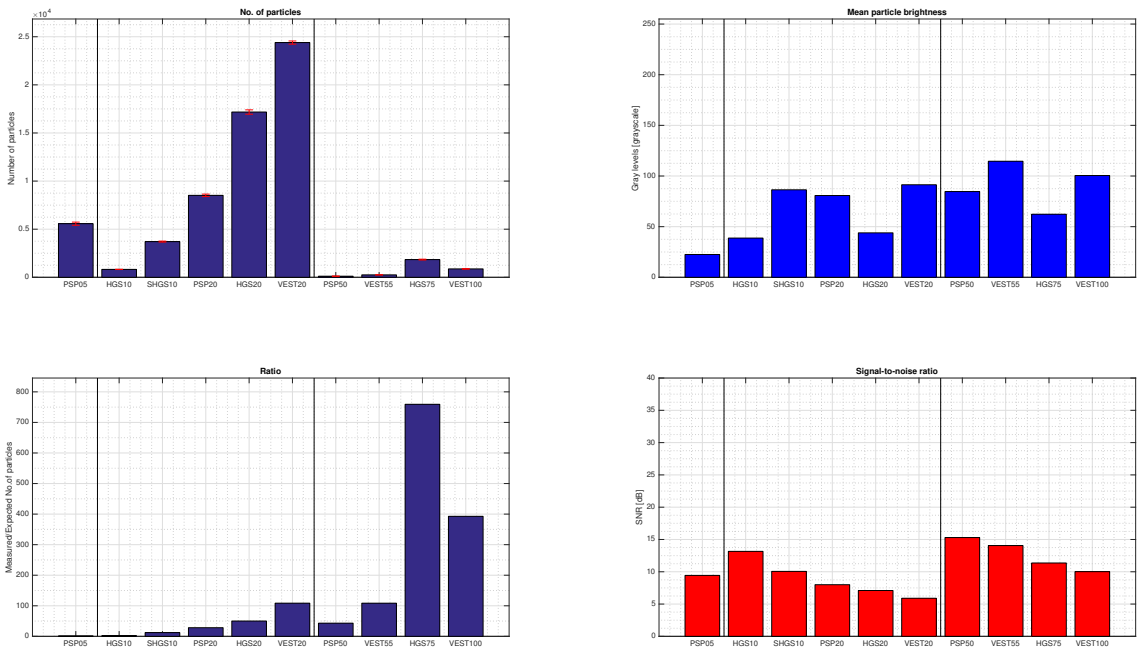

Figure 27 - Comparison of all particle sorts; Left upper chart shows results for 1,9W – rest of sub charts show mean averages for all laser power settings

Particles can be again divided, according to their mean brightness, into groups (from highest to lowest):

1. VEST55
2. VEST100
3. PSP20, VEST20, SHGS10, PSP50
4. HGS75
5. HGS20
6. HGS10
7. PSP05

Although there are some slight differences the order remains very similar as in the previous experiment. According to the expectations are brightest the biggest particles. The best properties seem to have VEST55, which in both experiments had the highest mean brightness around 110 units on the grayscale (i.e. of the maximum 255). For an unknown reason have VEST100 particles, although two times bigger, lower mean brightness and ended up behind VEST55. SHGS10 are because of their better reflecting properties ranked similarly as bigger particles such as PSP20 or VEST20.

Reason why there is such a difference in particle mean brightness of PSP50 between the previous experiment with 0,05g of seeding and this one with constant number

of particles could not be reasonably cleared. It is definitely worth some future measurements.

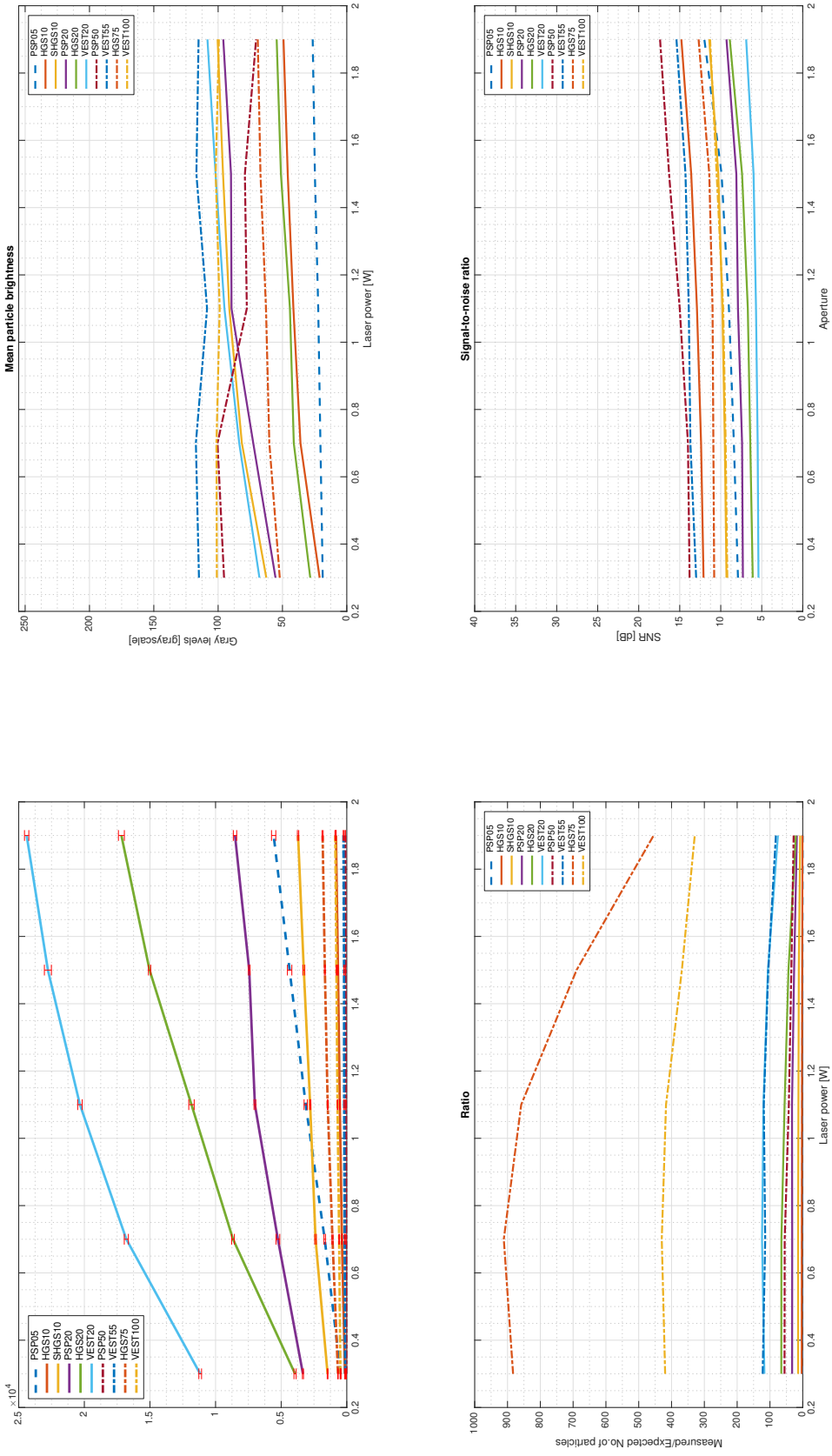

Figure 28 – Results for all particles in one image

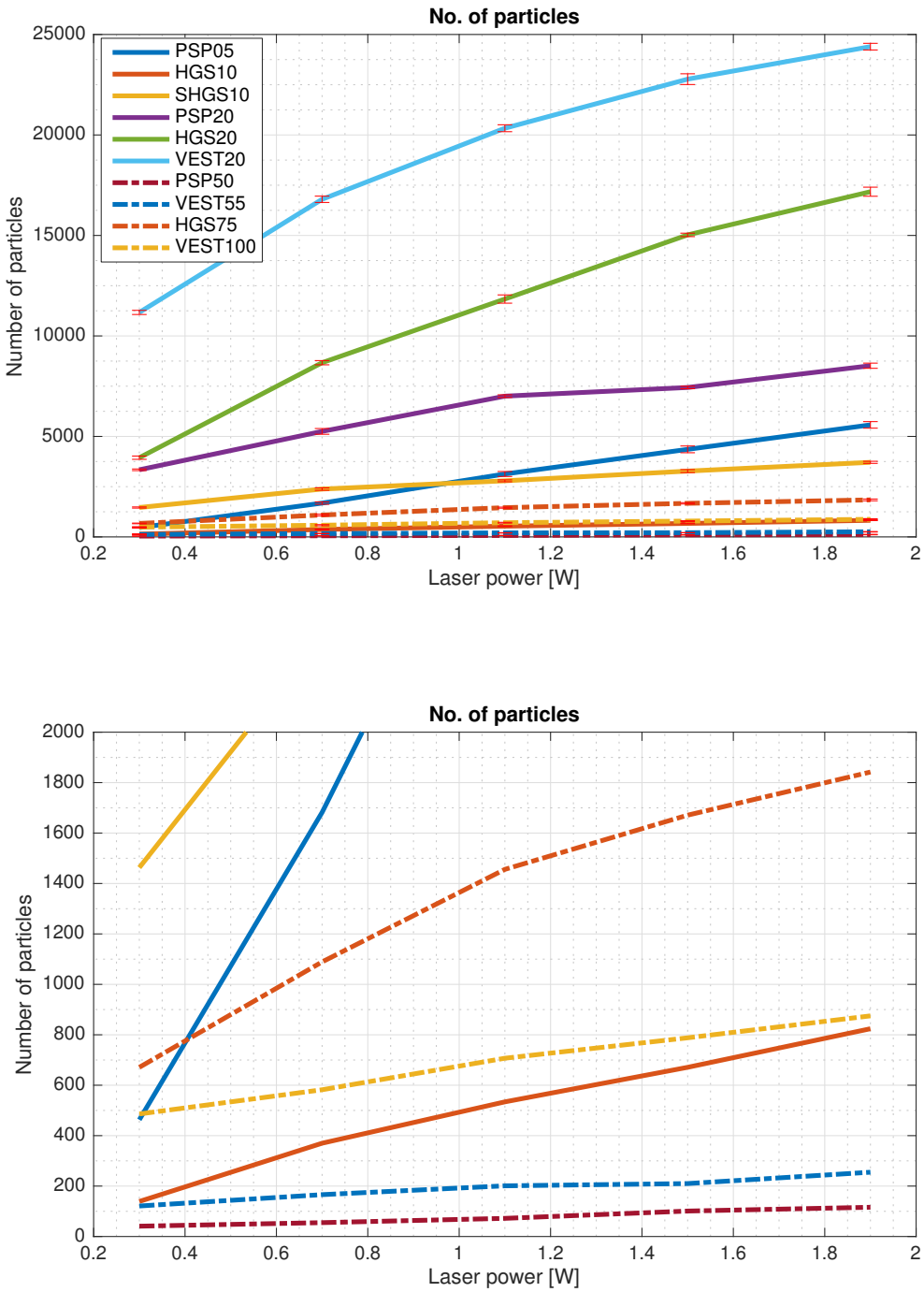

Figure 29 – Once again the left upper diagram from Figure 24 (above) and enlarged lower part of the same image (below)

On **Figure 29** are shown all the results together in one image. The results from the first group (PSP05) are shown in blue, from the second group in solid lines and from the third group in dashed lines.

4.3 Variations of Laser Thickness

The next experiment`s goal was to investigate how the results change with varying laser sheet thickness. Until that the laser sheet thickness had been constantly held at approximately 0,48 mm. In this experiment it was decided to set it to 1mm, 2mm and 4mm (wider thickness was not possible due to physical limitations of used optics).

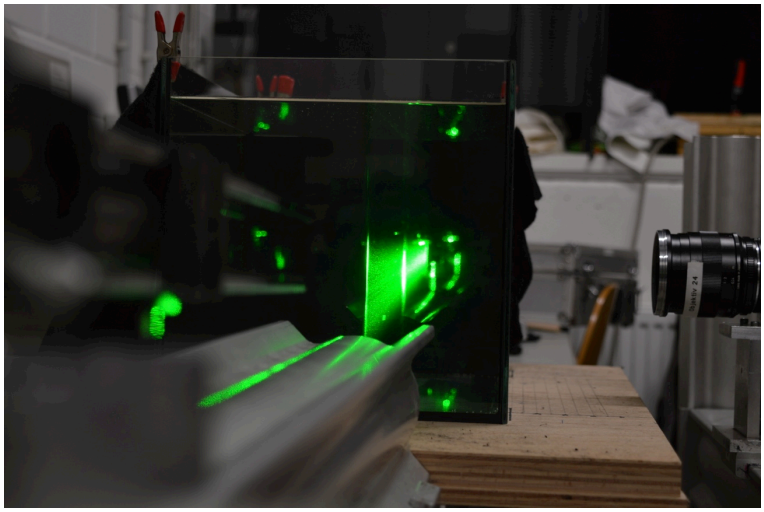

Figure 30 – Standard laser sheet thickness

According to expectations the number of particles increases nearly linearly with the increasing width (at least between the expansion from 1mm to 2mm), because the laser is directly and indirectly illuminating more particles. But with the wider laser sheet width also increases the area illuminated by the laser (sheet width x height) and since the laser power remains constant, the mean particle brightness decreases (Illuminance effect).

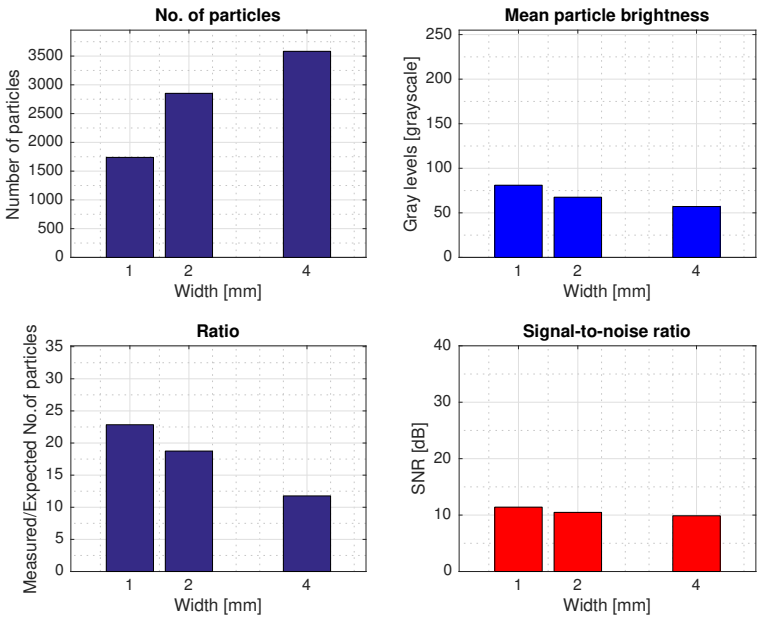

Figure 31 - Width variations for PSP20 (0,05g 1,9W): /1/- normal, /2/-double the size, /4/-four-times the size

4.4 Variations of AOI size

The goal was to investigate how a size of AOI can affect the results, in other words what might a moving of a camera nearer or further from the measured area cause. Normal size of AOI for all experiments was constantly set at 45x36 mm, which for the Carl Zeiss 50mm Macro Planar lens corresponds to approximately 15 cm of distance from the laser sheet. To enlarge the AOI the high-speed camera was moved backwards about 6 cm enlarging the AOI to 63x50 mm, which is almost a double of the previous size (1620 mm^2 to 3150 mm^2 = 195%). Camera could unfortunately not be moved forwards because of the vicinity of the aquarium`s glass. This would have been preferable, since there was a risk that moving the camera backwards might cause getting and unevenly bright image (because of limited laser sheet height). There was unfortunately no workaround possible at the time. Except focusing the lens no other changes were done. **Figure 32** shows the results for HGS20 particles.

Table 9 - AOI size and light density

Laser power [W]	Volume of standard AOI (45x36mm) [mm^3]	Laser light density [W/m^2]	Volume of enlarged AOI (63x50mm) [mm^3]	Laser light density [W/m^2]
0,4	777,70	6,2*10^-12	1512,19	8,6*10^-12
1,0	864,11	15,6*10^-12	1680,21	21,6*10^-12
1,5	950,52	23,3*10^-12	1848,23	32,4*10^-12
2,0	1123,34	41,5*10^-12	2184,28	57,6*10^-12

Despite of expectations the number of particles remained roughly the same, although AOI was virtually two times bigger. Also the mean particle brightness significantly decreased even though it should have remained the same.

Examination of raw images and analysed data revealed, that this is probably caused by a fact mentioned above, i.e. that moving camera backwards exposed the lower and upper part of the image regions with lower laser power than in the middle. Comparison of two raw images can be seen below (**Figure 33**).

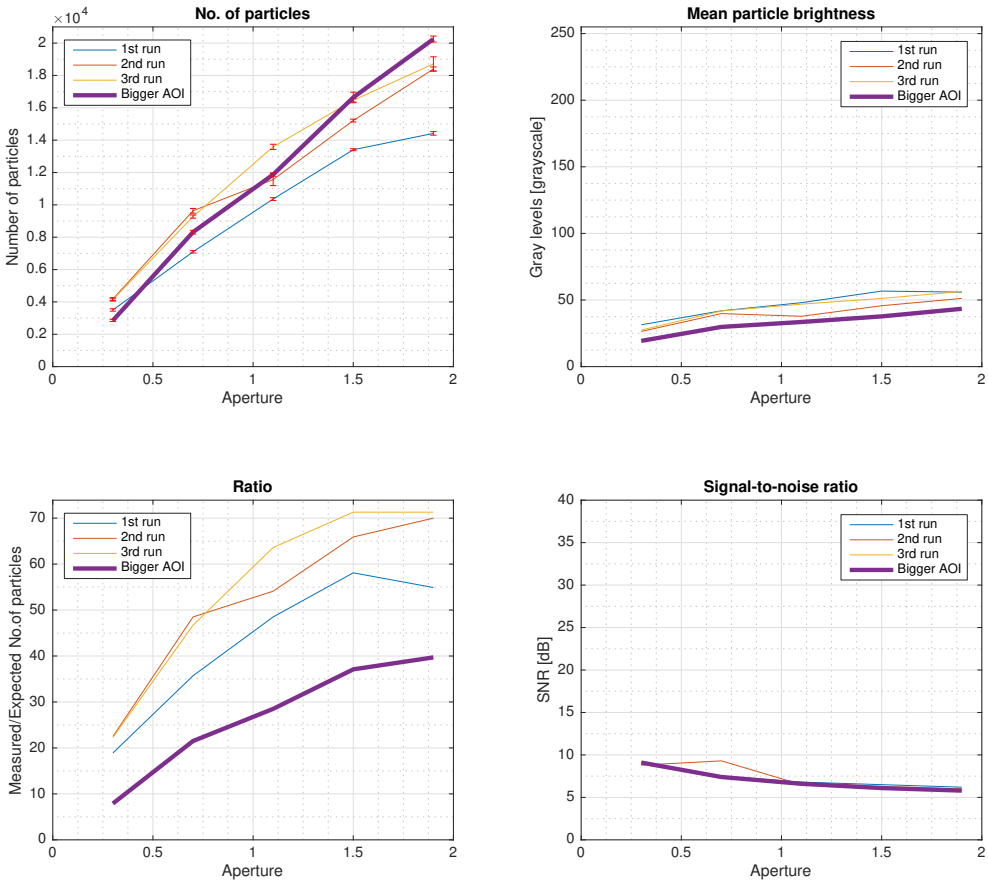

Figure 32 –HGS20, 3 measurements with normal AOI-45x36mm and larger AOI-63x50mm (in purple). 0,184g of seeding in the volume.

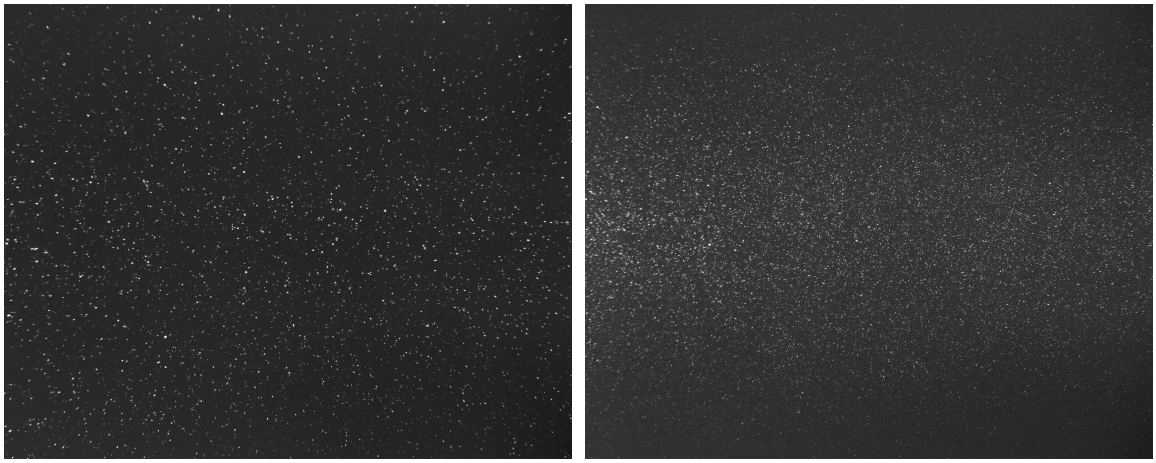

Figure 33 - Raw images captured during the experiment. Normal AOI (left) and enlarged AOI (right). Notice slightly darker regions in the upper part of the right image. (Both pictures with their brightness increased by 60%)

4.5 Variations of Viewing Angle

The next experiment aimed to test how varying the camera angle changes the particle images properties (all previous experiments were carried on under an constant angle of 90 degrees). To compensate for the angle, Scheimpflug adapter was mounted between the camera and the lens (**Figure 34**). With increasing tilt, another effect – astigmatism – was also influencing the measurements eventually limiting the maximum camera angle to ±40 degrees from the perpendicular axis. To increase the precision of data, exact alignment was controlled with a laser device and images were taken at increments of 5 degrees.

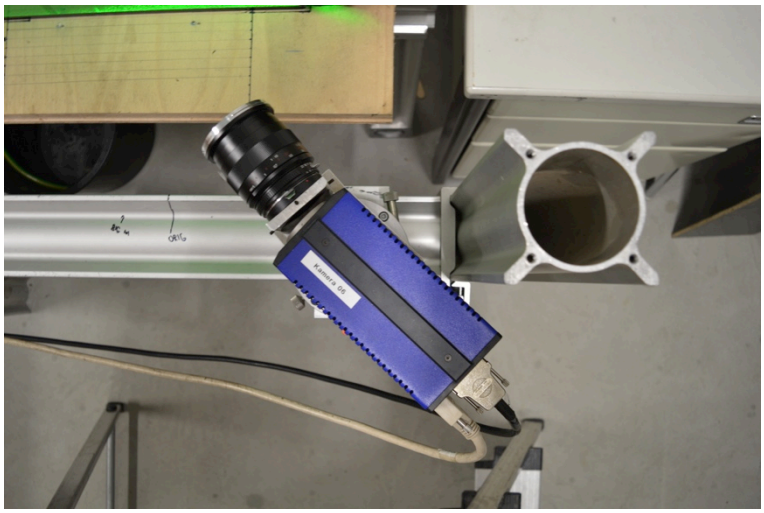

Figure 34 – Camera equipped with Scheimpflug adapter during measurements (For better visibility without the cover between adapter and lens)

Since the experiment was because of demands on precision time consuming it was realised for two particle sorts only – PSP20 and VEST100. As can be seen on **Figure 35** for PSP20, the Mean particle brightness is at 90 degrees at its maximum, decreasing with the changing angle. Rather constant SNR suggest, that the particles reflect less light in their vicinity, which causes a dimming of the background as well.

On the other hand, for very large particles – VEST100 (**Figure 36**) – is the Mean particle brightness by almost 1/3 higher and rather constant. Since is the SNR for both sorts almost the same, it suggests that in the case of VEST100 is not only the brightness of the particle images higher but also the background itself is brighter. These larger particles reflect more in their vicinity, which is in accordance with the previously measured and expected values.

According to the Mie theory described in **Chapter 2.4.2** should be the scattered intensity under 90 degrees the lowest, rapidly increasing with the changing angle. But the theory applies only for a scattering of a single particle, without taking into account the scattered light influencing other particles.

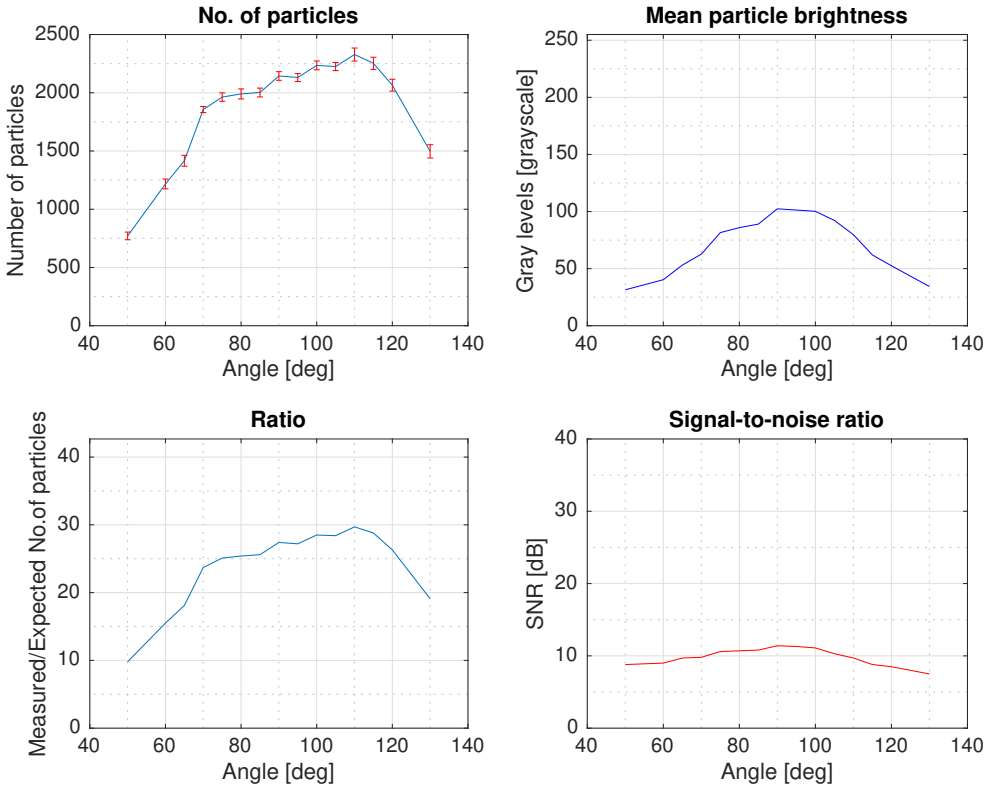

Figure 35 - Angle variation PSP20

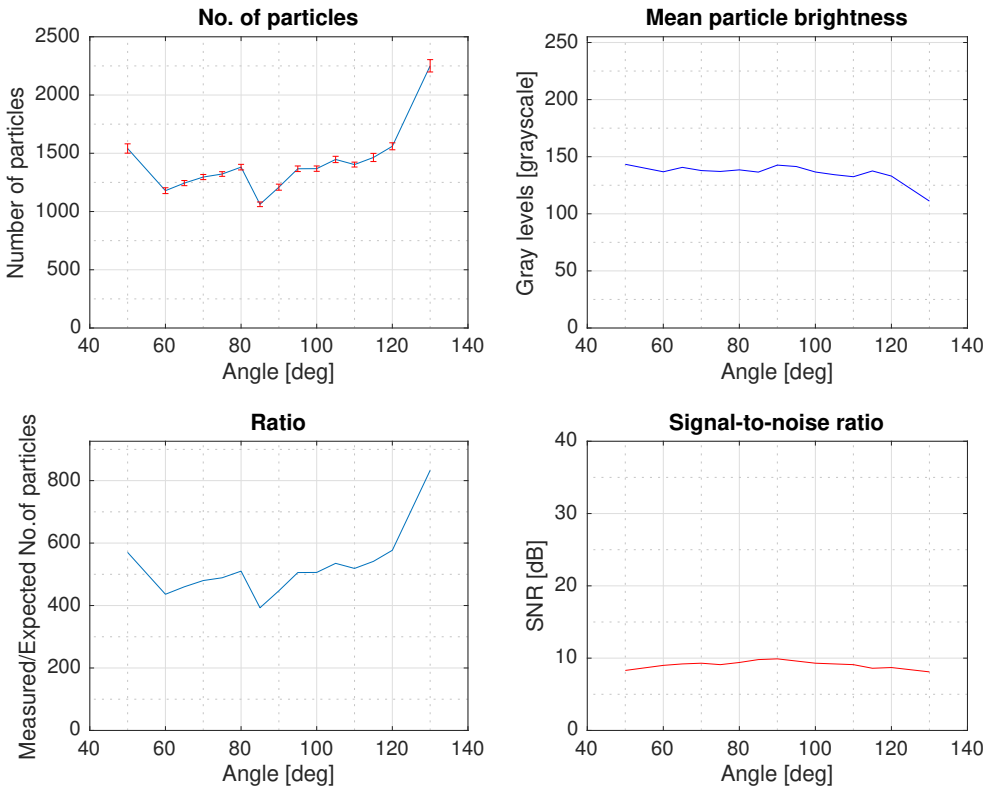

Figure 36 - Angle variation VEST100

4.6 Variations of Aperture Settings and Lenses

This experiment tested how different aperture settings and different lenses affect particle brightness. Three available types of lenses were used:

1. Carl Zeiss 2/50 mm *F2,0* Macro Planar Lens (*f-numbers: 2; 2,2; 4; 5,6; 8; 11; 16; 22*)
2. Carl Zeiss 2/100 mm *F2,0* Milvus Lens (*f-numbers: 2; 2,2; 4; 5,6; 8; 11; 16; 22*)
3. Tamron SP AF180mm *F/3,5* (*f-numbers: 3,5; 5,6; 8; 11; 16; 22*)

Since all three lenses have different focal lengths, the distance of a camera from the laser sheet had to be adjusted in order to achieve the same AOI size for all of them to make the results comparable. Aperture setting was stepwise adjusted within the whole aperture scale from 2,0 to 22 (or 3,5 – 22 in case of Tamron 180mm). **Figure 37** illustrates that for the same AOI size, even lens with longer focal length yields almost the same results as the 50 mm Carl Zeiss. They begin to return worse values first with higher f-numbers, but a need to use an f-number of 11 or more is probably a regime, which would in case of real PIV measurement highly unlikely happen.

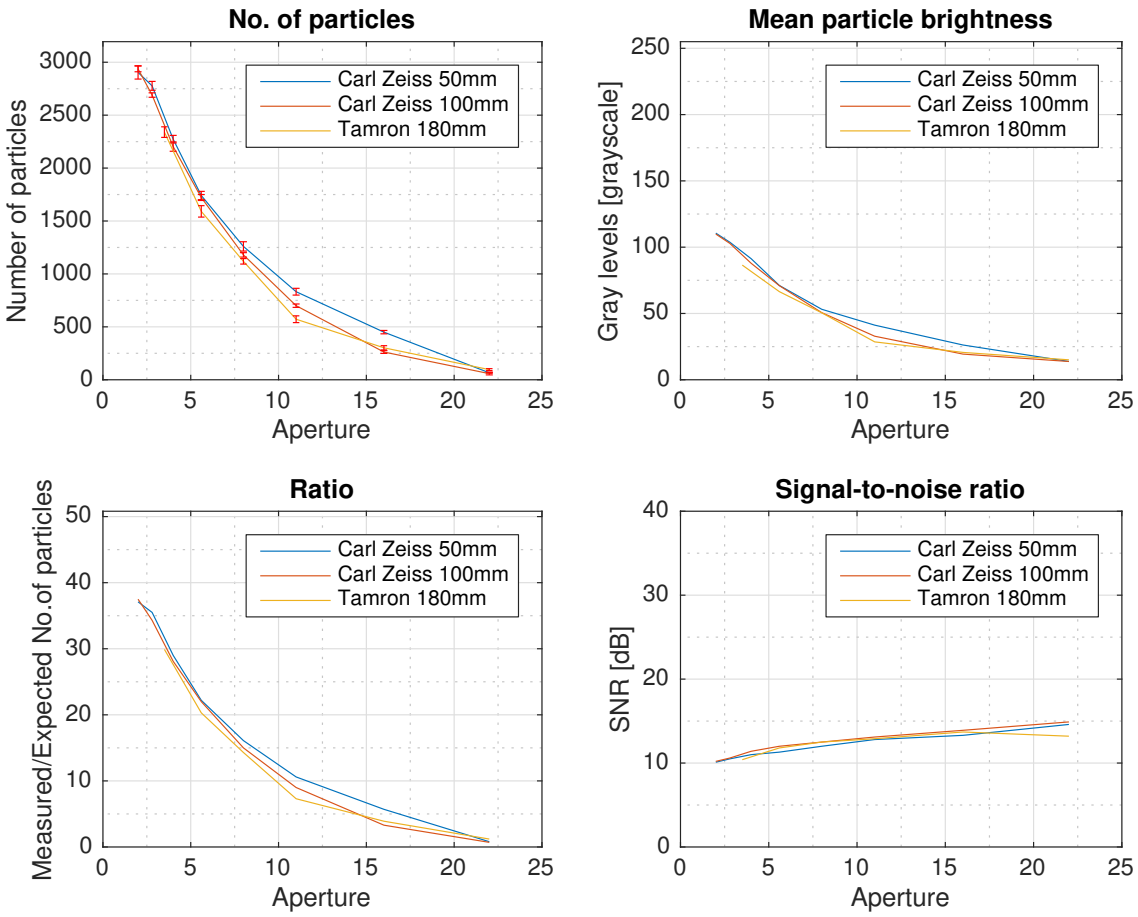

Figure 37 - All lenses for all aperture settings (PSP20 1,9W)

Figure 38 further illustrates the difference between the three lenses for f-number = 5,6 (the lowest common f-number of all), for each lens are always shown two independent experiments.

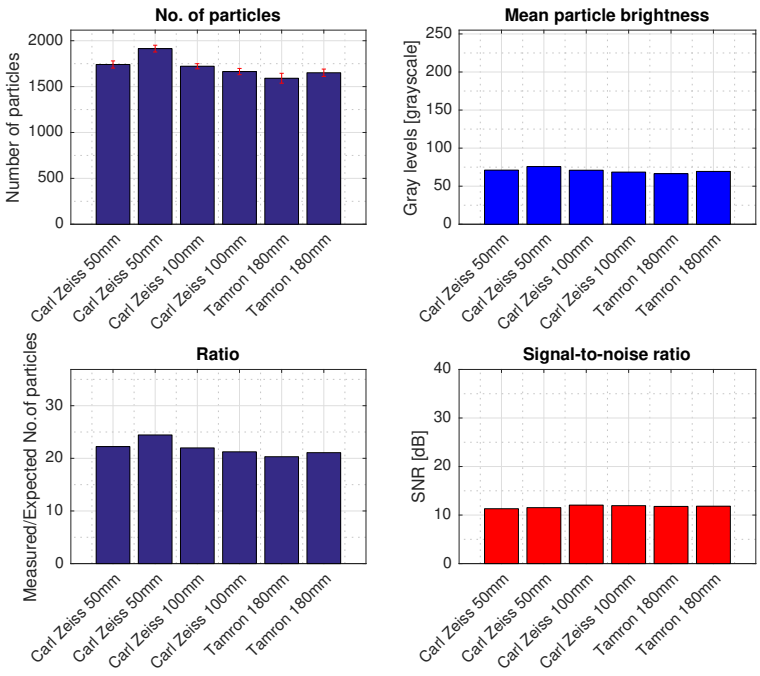

Figure 38 – All lenses – *f-number* 5,6 (PSP20 1,9W)

4.1 Variations of Concentration

This experiment examined the optical behaviour of the fluid with an increasing concentration of seeding for the constant laser power. As results on **Figure 39** show, number of measured particles increases all the time approximately linearly even though the fluid appeared to be “milky” since concentration of about 0,3g of PSP20 per 20,5 litre was reached). The Mean particle brightness shows a slight tendency to grow but eventually sink with rising concentration. On the other hand it must be noted, that the difference is almost at the edge of measurability. Decreasing SNR confirms the “milky” appearance of the fluid, i.e. increasing brightness of the background.

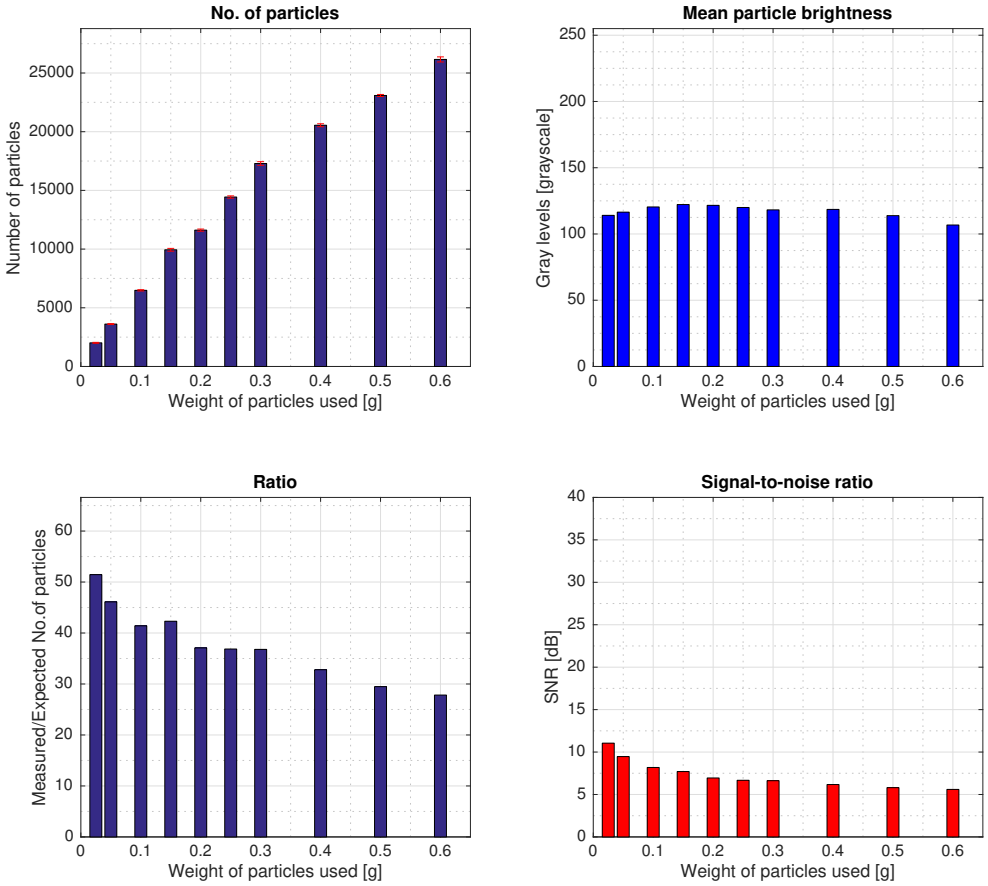

Figure 39 - Increasing concentration of PSP20 (1,9W)

4.2 Variations of Distance

This last experiment was aimed to study the behaviour of particle images if the volume, which the scattered light from a laser sheet towards the camera has to penetrate through water, increases. It was achieved as shown on **Figure 40** by step-wise moving the aquarium forwards and backwards while the rest of the setup remained stationary. The experiment was from one side limited by the decreasing distance between the lens and the aquarium glass, from the other side by keeping at some meaningful amount of water that the light had to penetrate.

As results from **Figure 41**, with a stepwise adding of seeding (increments of 0,05g) increases also the visible number of particles, as was also proven in the previous chapter. It pretty illustrates functionality of the picture analysis program used. All values linearly decrease with the increasing width of water between the camera and the laser sheet (there are some discrepancies visible, which might be caused by inaccuracy of measurements, but the trend is obvious). The Particle mean brightness on the contrary remains rather the same showing no development with changing width. SNR remains also practically the same. Fully with expectations it remains the highest for the least concentrated fluid and vice versa.

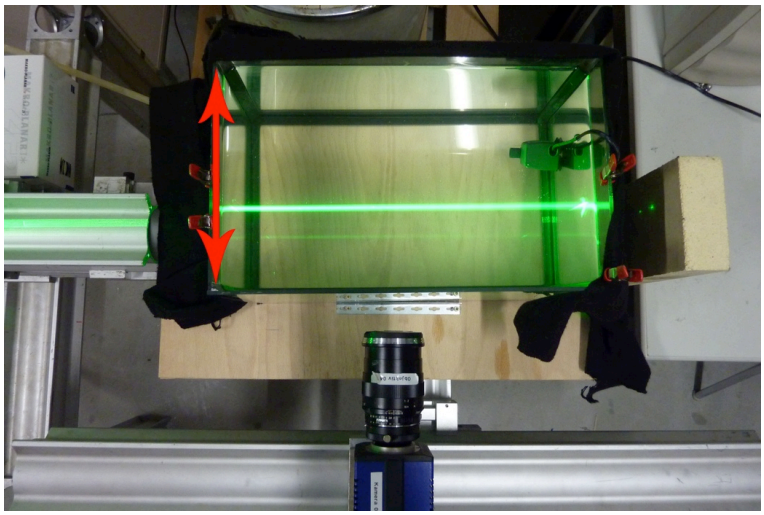

Figure 40 - The aquarium was moved forwards and backwards (red arrow), the rest of the setup was held static

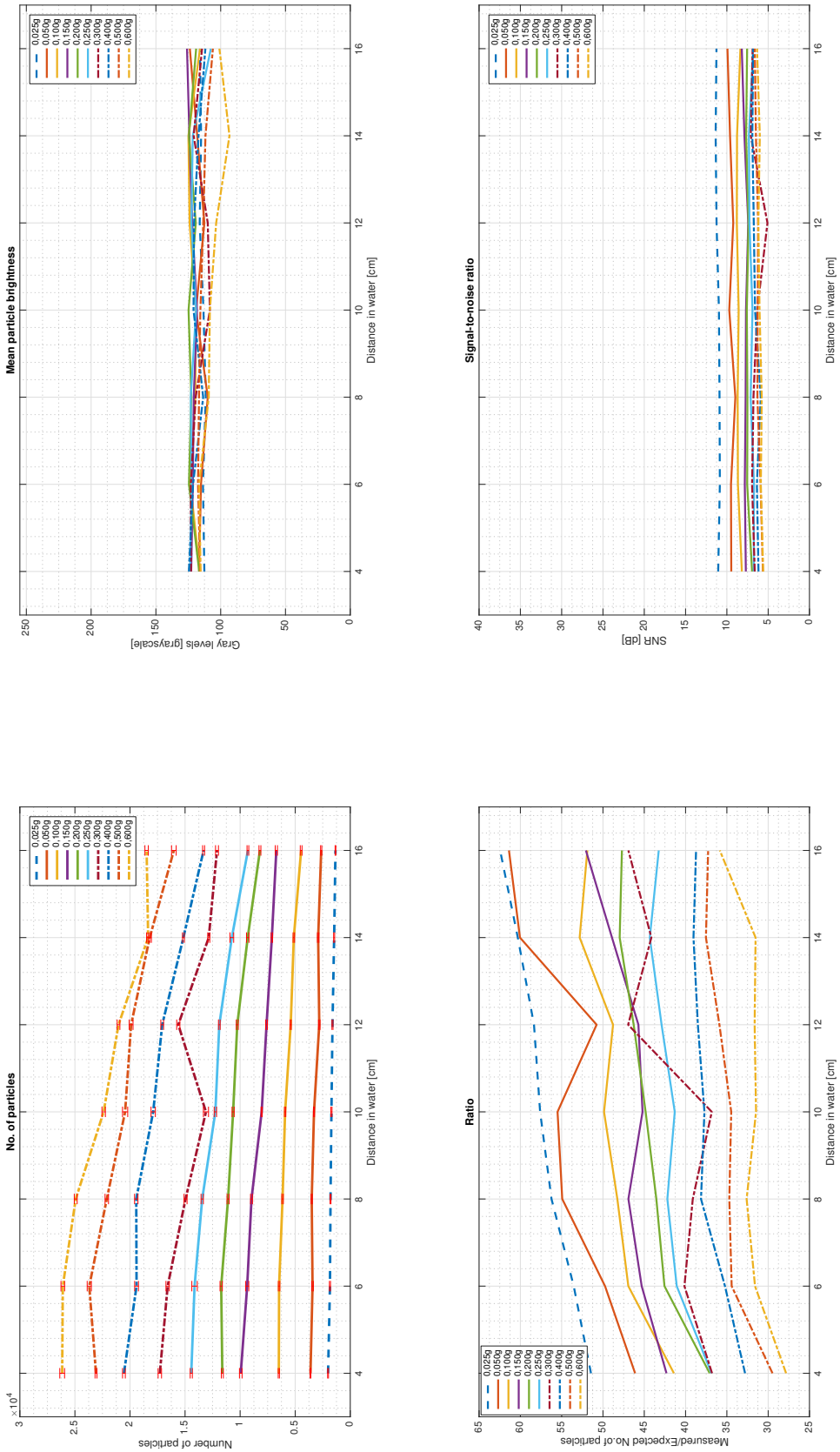

Figure 41 - Distance variation

5. Summary

Various sorts of particles were tested in this work in order to find factors defining the brightness of particle images in PIV-applications. Once the theory behind scattering of small particles was presented, pictures of all sorts of tracer particles were taken using a microscope to check their microscopic size and shape. This revealed, that many seeding sorts are rather "potato-shaped" than spherical and that their size can significantly vary from the average diameter. Using a test bed and a laser with a maximum power of 2,3W, numerous experiments were done to separately quantify all possible influence factors. These were: various laser power; various amount of seeding particles used; various laser sheet thickness; various size of area of interest (AOI); various camera angle; various aperture settings; various camera lenses used; various concentration of seeding particles and at last various depth of water between the camera and the laser sheet.

Answering the main question of this thesis – what sort of particles should be preferably used in PIV applications – is not an easy task. As previous chapters illustrate, there are many effects that have light or strong effect on brightness of individual particles and there are still many unanswered questions and problems, which emerged during experiments.

The overall best properties have, according to the results, particles *LaVision Vestosint 55µm* (referred to as VEST55). Their mean particle brightness was on an average by 20% higher than by other sorts. They were, surprisingly and against expectations, even brighter than their larger version Vestosint 100µm. This anomaly can be probably answered by the fact that Vestosint 100µm is, thanks to its size, already in a different scattering regime – a geometric optics regime (see a Chapter 2.4). This further reduces its scattering in direction of the camera. Mean particle brightnesses for Polyamide seeding particles 20µm (PSP20), Vestosint 20 µm and Silver coated hollow glass spheres 10µm were rather very similar. As was presented in Chapter 1 (all official list prices – stand January 2016; calculated for 100g if necessary):

100g of Vestosint costs 18,00 €,
100g of Hollow glass spheres 30,00 €,
100g of Polyamide seeding particles 65,60 €
100g of Silver coated hollow glass spheres 228,00 €

Under these circumstances it is clear, that Vestosint can be definitely recommended as the best option for PIV in water. Not only were results for this seeding overall the best,

but it is also the cheapest sort of all tested. Its only disadvantage is its higher density (1,2g/cm^3), compared to PSP (1,03g/cm^3) or HGS (1,1g/cm^3). Silver coated hollow glass spheres have, thanks to the used coating, the highest density of all – 1,4g/cm^3. According to the presented theory increases the intensity of the scattered light with the size of a particle. On the other hand, as was also shown, with a greater diameter increases the velocity lag. User should therefore always keep this in mind and choose the appropriate particles according to the planned experiment.

Increasing the laser sheet width proved (as expected according to the theory) to increase the number of visible particles. However, it is desired to keep it rather as thin as possible during a PIV experiment in order to focus on a flow along the longitudinal axis only.

Experiment with the different size of AOI is definitely worth another measurements. Using another lens with a bigger aperture would increase the previously limiting distance between the camera and the glass - so it would be possible to enlarge and even reduce the size of the AOI bringing more detailed results.

Experiment with different lenses proved them not to have much influence (if any) on results, assuming that the AOI size is held constant and the same aperture is used.

In the experiment with over-seeded water or increased distance between the laser sheet and the camera it was expected that numerous particles “blocking the way” might reduce the mean particle brightness. But results proved that particles tend to maintain the same brightness even under these circumstances (although the number of particles increased distinctively in the end of the experiment by 25 times). The same brightness remained even with a higher distance between the laser sheet and the camera.

5.1 Ideas for Future Work

During the analysis of data reappeared some old and appeared some new, unanswered questions, which would definitely be worth further experiments.

Laser polarization effects. The scattering efficiency strongly depends on polarisation of the incident wave. Safety glass used for the water tunnel also tends to refract the incident light according to the wave polarisation so it would be meaningful to examine this behaviour further for different polarisations and viewing angles. [1]

Proper dispersion of particles and particle clusters. Seeding tends to hold together in small clusters so suitable mechanisms to distribute it evenly within the volume are vital for good results.

Improving the analysis software in order to get more precise results. Determination of brightness of each particle can be done by analysis of its peak brightness level. This method would be definitely more time consuming, would lay higher demands on computer performance and would require some advanced programming skills, but is definitely worth the invested time.

During the experiment with a varying camera angle, an astigmatism effect had strongly limited the variety of angles to ±40 degrees from the perpendicular axis. Use of triangular prism made of glass attached to the sidewall of the aquarium could have reduced this phenomena and allowed good results even under sharp angles.

5.2 PIV as a research tool for Aviation

PIV has slowly become a very useful tool for aerodynamics` engineers in aviation or automotive industry. It is preferred for its very clear visualisation and interpretation of measured data. Since 2015 have engineers at the Institute of Fluid Mechanics at TU Braunschweig run experiments with a generic airfoil with a plain flap (60°). It is a part of a German project SFB880 “Fundamentals of High-Lift for future commercial Aircraft”, which main tasks are: use of shorter runways, moving airfields closer to the cities and reaching of cruising level faster. All these should together collaborate on reduction of environmental burden. One of the tools is better understanding of high-lift airfoils and more efficient high-lift. [16]

All these experiments have been done in a water tunnel using a PIV as a visualisation tool. In order to properly seed the water, large amounts of tracer particles must be used. To minimize costs and for better understanding of all influence factors, this thesis tried to evaluate them separately and to quantify their influence.

Although the results of this thesis are not to be used directly in aviation industry, they aim to help engineers to maximize the output of their research by receiving the best results when using PIV.

6. List of Acronyms

AOI	Area Of Interest
HGS	Hollow Glass Spheres or Glass Hollow Spheres
Pixel, Px	Acronym derived from PICture ELement. It is a single cell on a digital sensor. In a grayscale image, each pixel is associated with a numerical intensity value describing the local gray value or colour
PSP	Polyamide Seeding Particle(s) (particles based on Polyamide 12)
PTU	Programmable Timing Unit
SNR	Signal-to-noise Ratio
VEST	Vestosint (particles based on Polyamide 12)

7. References

1. RAFFEL, M. et al. *Particle Image Velocimetry: A practical guide*. Second Edition. Berlin: Springer, 2007.

2. Dantec Dynamics. *Seeding materials* [online]. Dostupné také z: http://www.dantecdynamics.com/seeding-materials

3. VESTOSINT.COM. *VESTOSINT Polyamide 12 Coating Powders*. VESTOSINT-polyamide-12-coating-powders-EN.pdf.

4. Evonik Industries. *About Vestosint* [online]. Dostupné také z: http://www.vestosint.com/product/vestosint

5. Pegasus Lasersysteme. *Pegasus High power 532nm DPSS Laser* [online]. Dostupné také z: http://www.pegasus-lasersysteme.de/index_htm_files/DS%20PLUTO-F%20Series.pdf

6. HULST, H. C. V. D. *Light Scattering by Small Particles*. 2nd Edition. Courier Corporation, 1957, 470 s..

7. DULLEMOND. Universität Heidelberg. In: *Chapter 6 - Dust scattering of particles* [online]. 15. 12. 2015. Dostupné také z: http://www.ita.uni-heidelberg.de/~dullemond/lectures/radtrans_2012/Chapter_6.pdf

8. Refractive index database [online]. [cit. 2015-12-10]. Dostupné z: http://refractiveindex.info

9. ZHONG, M. *Light scattering by small particles.pdf* [Web presentation]. 2. dubna 2010.

10. BORHEN, C. F. a D. R. HUFMAN. *Absorption and Scattering of Light by Small Particles*. Wiley, 1983.

11. Shimadzu corp. *Measurement of Solar Transmittance through Plate Glass* [online]. [cit. 2015-12-15]. Dostupné z: http://www.shimadzu.com/an/industry/ceramicsmetalsmining/chem0501005.htm

12. Wikipedia. *Cleanroom* [online]. [cit. 2015-12-24]. Dostupné z: https://en.wikipedia.org/wiki/Cleanroom

13. ANALYST, I. Matlabcentral. In: *recurse_subfolders.m* [online]. 14. 02. 2014 [cit. 2016-01-05]. Dostupné z: http://de.mathworks.com/matlabcentral/answers/uploaded_files/8072/recurse_subfolders.m

14. CASPER, M. et al. Qualification of oil-based tracer particles for heated Ludwieg tubes. 2014, č. 55.

15. Wikipedia. *Signal-to-noise ratio (imaging)* [online]. [cit. 2016-01-12]. Dostupné z:

https://en.wikipedia.org/wiki/Signal-to-noise_ratio_(imaging)

16. TU Braunschweig. In: *Kurzdarstellung Sonderforschungsbereich 880 - Grundlagen des Hochauftriebs künftiger …* [online]. 2011 [cit. 2016. Dostupné z: https://www.tu-braunschweig.de/Medien-DB/ism/sfb880_kurzvorstellung.pdf

17. UNIVERSITY AT BUFFALO. University at Buffalo. In: *Lecture Seeding Particle for PIV* [online]. Dostupné také z: www.eng.buffalo.edu/Courses/mae513/Lecture__Seeding_Particle_for_PIV.ppt

18. *Wikimedia commons* [online].

8. List of Figures

9. List of Tables